iScience

CellPress

Article

The Introduction of the Radical Cascade Reaction into Polymer Chemistry: A One-Step Strategy for Synchronized Polymerization and Modification

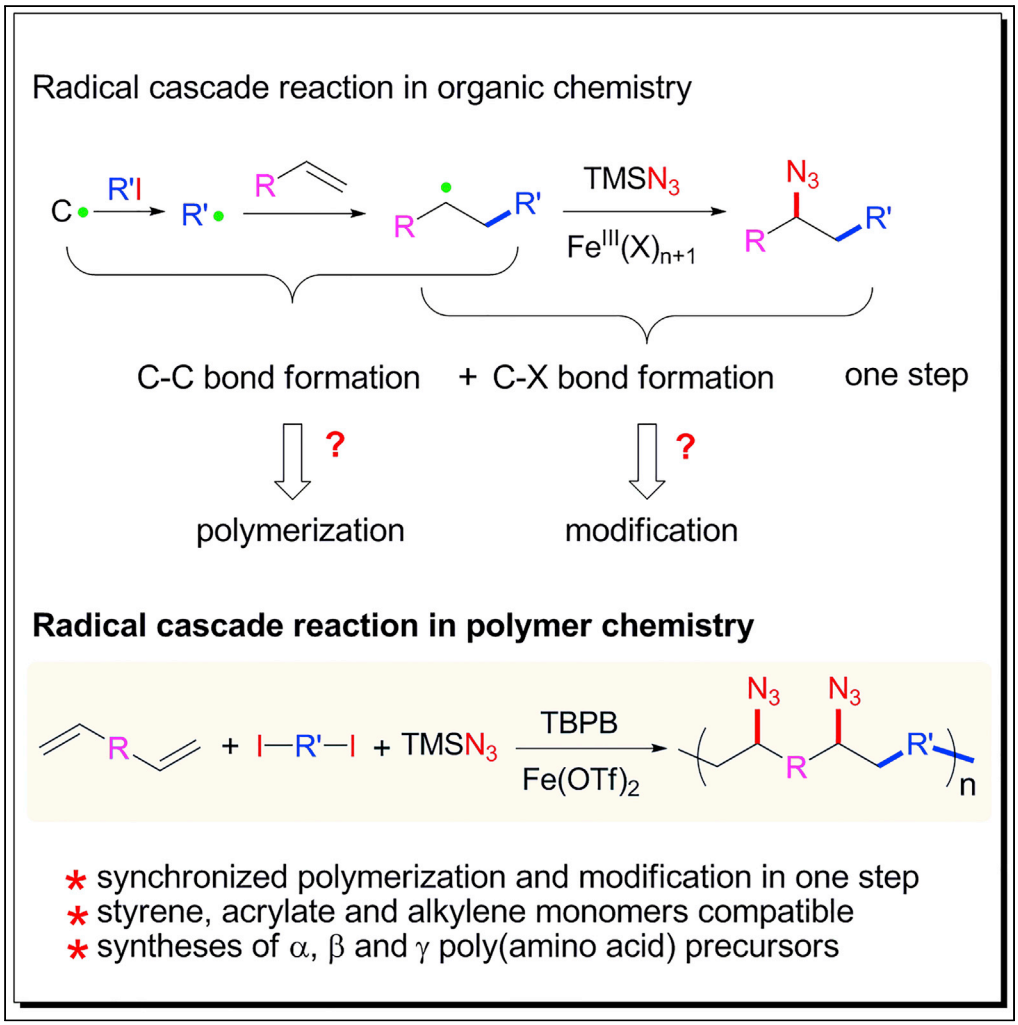

Nengbo Zhu, Mong-Feng Chiou, Haigen Xiong, ..., Yajun Li, Wen-Ming Wan, Hongli Bao

wanwenming@fjirsm.ac.cn (W.-M.W.)
hlbao@fjirsm.ac.cn (H.B.)

HIGHLIGHTS

Synchronized polymerization and modification

Radical cascade polymerization

Alkene functionalization polymerization

Zhu et al., iScience *23*, 100902 March 27, 2020
https://doi.org/10.1016/j.isci.2020.100902

iScience

CellPress

Article

The Introduction of the Radical Cascade Reaction into Polymer Chemistry: A One-Step Strategy for Synchronized Polymerization and Modification

Nengbo Zhu,[1] Mong-Feng Chiou,[1] Haigen Xiong,[1] Min Su,[1] Muqiao Su,[1] Yajun Li,[1] Wen-Ming Wan,[1,*] and Hongli Bao[1,2,*]

SUMMARY

Polymerization and modification play central roles in polymer chemistry and are generally implemented in two steps, which suffer from the time-consuming two-step strategy and present considerable challenge for complete modification. By introducing the radical cascade reaction (RCR) into polymer chemistry, a one-step strategy is demonstrated to achieve synchronized polymerization and complete modification *in situ*. Attributed to the cascade feature of iron-catalyzed three-component alkene carboazidation RCR exhibiting carbon-carbon bond formation and carbon-azide bond formation with extremely high efficiency and selectivity in one step, radical cascade polymerization therefore enables the *in situ* synchronized polymerization through continuous carbon-carbon bond formation and complete modification through carbon-azide bond formation simultaneously. This results in a series of α, β, and γ poly(amino acid) precursors. This result not only expands the methodology library of polymerization, but also the possibility for polymer science to achieve functional polymers with tailored chemical functionality from *in situ* polymerization.

INTRODUCTION

Synthetic polymer materials with desired functionalities in the form of plastics, fibers, rubbers, etc., have played significant roles in human life since last century, which rely mainly on the prosperous development of polymerization and modification methodologies. Polymerization and modification are two fundamental aspects of polymer chemistry and have played central roles in the history of polymer chemistry (Matyjaszewski and Xia, 2001; Kamigaito et al., 2001; Gauthier et al., 2009; Boaen and Hillmyer, 2005; Richards et al., 2012; Britovsek et al., 1999; Moad et al., 2005; Sun et al., 2013). Generally, polymer modification can be implemented either during the monomer synthesis or by post-polymerization modification (Scheme 1A) (Wan et al., 2014, 2017; Lv et al., 2017; Gao et al., 2014; Kakuchi and Theato, 2013; Hedir et al., 2015; Wang et al., 2017b). However, these broadly applied two-step strategies have many disadvantages including time consumption, waste of resources, and solubility issues. And complete post-polymerization modification is a considerable challenge owing to the reduced reactivity of functional groups on the polymer chain and the embedding as well as the shielding effect of the polymer chain on functional groups. We questioned whether a one-step strategy can be developed to overcome the disadvantages by realizing synchronized polymerization and modification in one step, constructing and modifying a polymer simultaneously. To develop a one-step strategy to implement polymerization and modification will enable step-economy and efficient complete modification and is therefore highly desirable.

The introduction of organic reactions to polymer chemistry has received considerable research effort for its convenient and versatile effect on the development of new polymerization methodologies. However, not all organic reactions are potential candidates for the design of new polymerization methodology. Only highly efficient and selective organic reactions are suitable to be introduced into polymer chemistry to develop new polymerization methodology. For example, atom transfer radical addition reaction (Wang and Matyjaszewski, 1995; Pintauer and Matyjaszewski, 2008), radical addition-fragmentation reaction (Moad et al., 2008; Chiefari et al., 1998), olefin metathesis reaction (Vougioukalakis and Grubbs, 2010; Bielawski and Grubbs, 2000, 2007), Suzuki coupling reaction (Miyaura et al., 1981; Littke et al., 2000; Kotha et al., 2002; Schluter, 2001; Yokoyama et al., 2007; Baggett et al., 2015), Michael addition reaction (Liu et al., 2003; Wang et al., 2005), Stille coupling reaction (Bao et al., 1995; Littke and Fu, 1999; Yin et al., 2016; Guo et al., 2014), click chemistry reactions (He et al., 2016, 2017), multiple components reactions

[1]Key Laboratory of Coal to Ethylene Glycol and Its Related Technology, State Key Laboratory of Structural Chemistry, Center for Excellence in Molecular Synthesis, Fujian Institute of Research on the Structure of Matter, Chinese Academy of Sciences, 155 Yangqiao Road West, Fuzhou, Fujian 350002, P. R. of China

[2]Lead Contact

*Correspondence: wanwenming@fjirsm.ac.cn (W.-M.W.), hlbao@fjirsm.ac.cn (H.B.)

https://doi.org/10.1016/j.isci.2020.100902

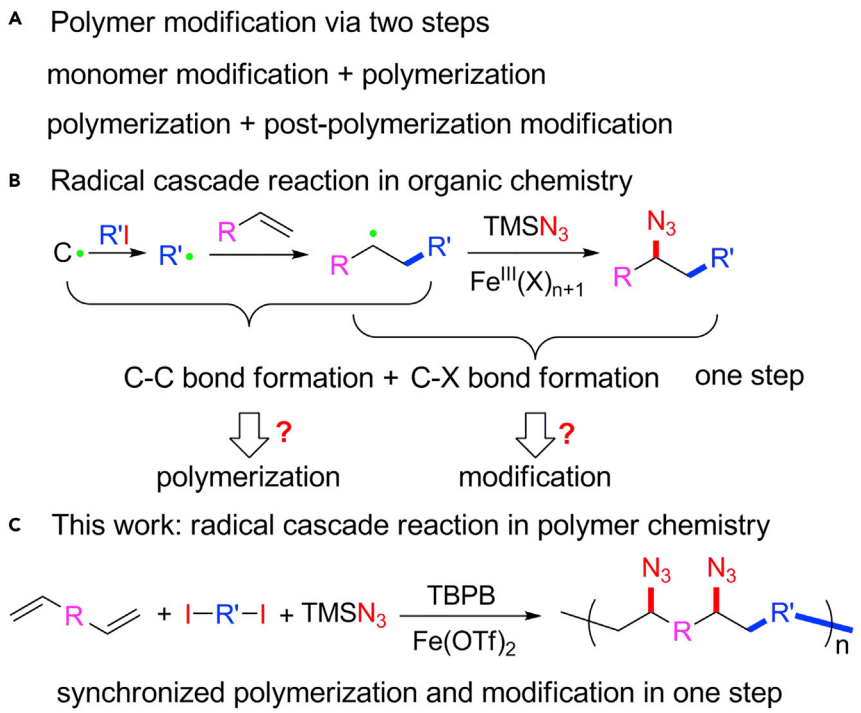

Scheme 1. The Introduction of Radical Cascade Reaction into Polymer Chemistry toward Synchronized Polymerization and Modification in One Step

(A) Polymer modification methods. (B) The highly efficient and selective iron-catalyzed three-component alkene carboazidation is used as an example of radical cascade reaction in organic chemistry. (C) Radical cascade polymerization through alkene functionalization polymerization.

(Deng et al., 2012, 2016; Kreye et al., 2011; Wei et al., 2017; Wu et al., 2017; Xue et al., 2016), Barbier reaction (Sun et al., 2017; Jing et al., 2019) etc. have been successfully introduced into polymer chemistry to develop desired polymerization methodologies (Tebben and Studer, 2011; Jiang et al., 2018; Huang et al., 2019; Liu et al., 1999). These polymerization methodologies have expanded the structure and functionality library of polymer chemistry in the past decades. The introduction of highly efficient and selective organic reactions into polymer chemistry is therefore highly desirable for polymer science.

Radical cascade reactions (RCRs) are cascade reactions involving two or more radical procedures and bond formation. They have attracted considerable interest in modern organic synthesis for their versatility in alkene addition and functionalization (Brill et al., 2016; Plesniak et al., 2017; Wang et al., 2017, 2018; Xiong et al., 2019; Yu et al., 2018; Zhang and Studer, 2015). Attributed to the cascade feature of RCR, they feature the chemical procedure of carbon-carbon bond and complete carbon-X (functional moieties including azide, amine, hydroxide) formation in one step (Scheme 1B). We therefore hypothesize that the exploration of RCR exhibiting extremely high efficiency and selectivity on formation of carbon-carbon and carbon-X bonds and its introduction into polymer chemistry will enable the polymerization through continuous carbon-carbon bond formation and complete modification through carbon-X formation in a single step.

Herein, we demonstrate the introduction of iron-catalyzed three-component alkene carboazidation RCR into polymer chemistry to develop radical cascade polymerization (RCP) through alkene functionalization polymerization, a novel polymerization methodology. This iron-catalyzed three-component alkene carboazidation RCR exhibits extremely high efficiency and selectivity in the formation of carbon-carbon and carbon-azide bonds. Attributed to its efficiency, selectivity, and cascade feature, this RCP enables the polymerization and complete modification in one step. For better understanding the versatility of RCP methodology, RCP polymers are further demonstrated as α, β, and γ amino acid polymer precursors. This work therefore not only expands the methodology library of polymerization, but also opens a window for polymer science to achieve polymer materials with tailored chemical functionality from *in situ* polymerization.

Entry	Substrate	Product	Conv. (%)[a]	Mn[b]	Mw[b]	PDI[b]
1		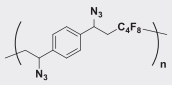	99	5,100	9,100	1.78
2		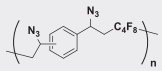	99	4,300	6,600	1.53
3	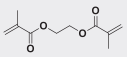	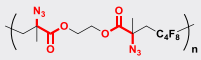 Poly(α-amino acid) Precursors	98	3,000	4,400	1.47
4	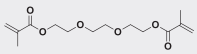	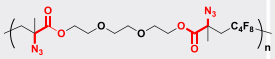 Poly(α-amino acid) Precursors	98	4,200	5,700	1.36
5[c]	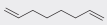	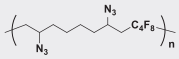	97	3,400	5,400	1.59
6	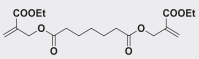	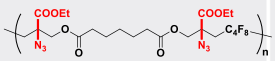 Poly(β-amino acid) Precursors	99	6,800	11,700	1.72
7[d]	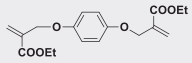	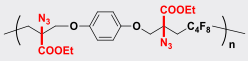 Poly(α-amino acid) Precursors	99	–[e]		
8[d]	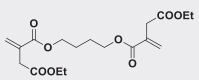	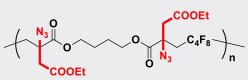 Poly(β-amino acid) Precursors	99	7,800	13,700	1.76
9[d]	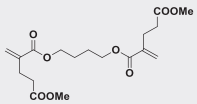	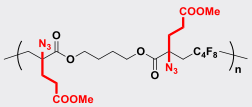 Poly(γ-amino acid) Precursors	98	4,600	7,200	1.57

Table 1. The Alkene Structures and Results of Polymers Synthesized by Radical Cascade Polymerization

Reaction conditions: alkene (1mmol, 1.0 eq.), $IC4F_8I$ (1.0 eq.), $TMSN_3$ (2.5 eq.), TBPB (3.0 eq.), $Fe(OTf)_2$ (5 mol%) and DME (1 mL), r.t, 40 h.

[a]Calculated from ^1H NMR spectroscopy.

[b]Measured by GPC.

[c]$TMSN_3$ (4.0 eq.), TBPB (5.0 eq.), 70°C.

[d]50°C.

[e]Not very soluble.

RESULTS AND DISCUSSION

According to our previous work, iron-catalyzed three-component carboazidation of alkenes is an RCR involving alkenes, azidotrimethylsilane ($TMSN_3$). and iodides. It shows high efficiency and selectivity in the formation of carbon-carbon and carbon-azide bonds, resulting in azides containing functional compounds or amino acids precursors when R or R′ contain ester groups (Scheme 1B). (Xiong et al., 2019) In this three-component RCR, cascade radical reactions take place via iron-catalyzed radical generation, iodine atom transfer, radical addition, and iron-catalyzed azido group transfer, producing carbon-carbon bond formation and carbon-azide bond formation. The iodide and $TMSN_3$ serve as carbon and azide

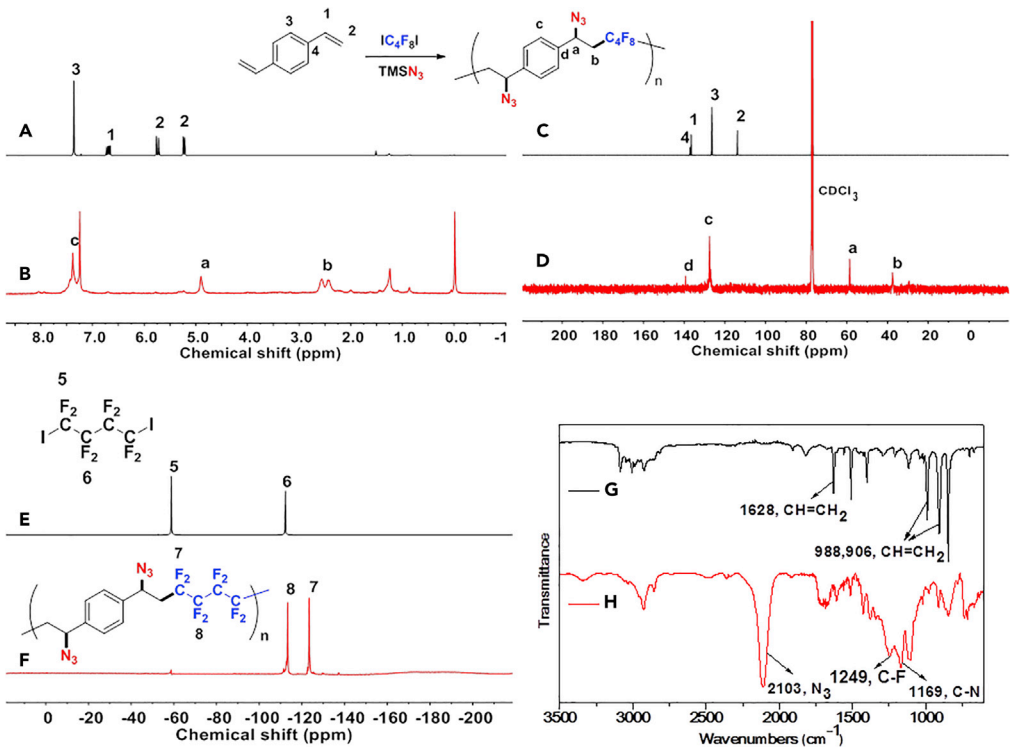

Figure 1. Radical Cascade Polymerization of an Alkene Through Alkene Functionalization Polymerization

1,4-Diiodoperfluorobutane ($IC4F_8I$) and azidotrimethylsilane ($TMSN_3$) were used as monomers. Reaction conditions: alkene (1 mmol, 1.0 eq.), $IC4F_8I$ (1.0 eq.), $TMSN_3$ (2.5 eq.), TBPB (3.0 eq.), $Fe(OTf)_2$ (5 mol%), and DME (1 mL), r.t, 40 h.

(A and B) ^{1}H NMR spectra (A: alkene; B: polymer).

(C and D) ^{13}C NMR spectra (C: alkene; D: polymer).

(E and F) ^{19}F NMR spectra (E: 1,4-diiodoperfluorobutane; F: polymer).

(G and H) FTIR spectra (G: alkene; H: polymer).

sources. In the hypothesis of RCP by introducing RCR into polymer chemistry to realize synchronized polymerization and modification, RCR candidates should show high efficiency and selectivity. This highly efficient and selective carbon-carbon bond formation can avoid other carbon source contamination that may terminate polymerization, whereas that of carbon-azide bond formation can avoid the radical polymerization of alkene by itself.

To prove the above hypothesis of introducing iron-catalyzed three-component alkene carboazidation RCR into polymer chemistry to realize synchronized polymerization and modification in one step, the A_2+B_2 type RCP was therefore designed with dienes, 1,4-diiodoperfluorobutane, and $TMSN_3$ as three-component monomers; iron(II) trifluoromethanesulfonate ($Fe(OTf)_2$) as catalyst; and *tert*-butyl peroxybenzoate (TBPB) as a radical initiator (Scheme 1C). To verify the above attempt to introduce RCR into polymer chemistry, iron-catalyzed RCPs were carried out in 1,2-dimethoxyethane (DME). A series of azide-containing polymers were successfully synthesized and are shown in Table 1. Taking the RCP of a diene monomer, 1,4-divinylbenzene as an example, its successful RCP was verified by NMR and Fourier transform infrared spectroscopy (FTIR) spectra (Figure 1). From ^{1}H NMR spectra shown in Figures 1A and 1B, the product shows broader peak signals in comparison with the sharp peak signals from the monomer, which is a typical phenomenon associated with polymerization. The successful polymerization can be further verified by the disappearance of signals from the vinyl group at 6.70, 5.72, and 5.24 ppm and the appearance of signals for carbon-carbon bond formation at 2.62–2.36 ppm and carbon-azide bond formation at 4.90 ppm in the ^{1}H NMR spectra (Figures 1A and 1B). From the ^{13}C NMR spectra shown in Figures 1C and 1D, the polymerization is verified by the disappearance of signals from the vinyl group at 136.49 and 113.78 ppm and the appearance of signals for carbon-carbon bond formation at 37.59 ppm and carbon-azide bond formation at 58.62 ppm. From the ^{19}F NMR spectra shown in Figures 1E and 1F, the signal at −58.82 ppm (CF_2-I) disappeared and a signal appeared at −123.34 ppm (CF_2-CH_2) after polymerization. From the FTIR spectra

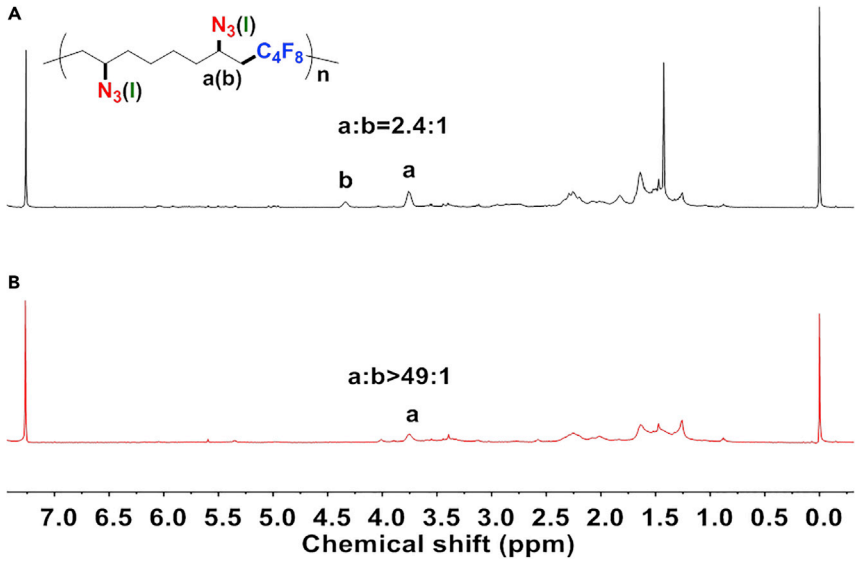

Figure 2. Controlled Azide/Iodine Modification of Resulting Polymers via One-Step RCP

(A) $Fe(OTf)_2$ (5 mol%), $TMSN_3$ (1.5 eq.), TBPB (3.0 eq.), 40°C.

(B) $Fe(OTf)_2$ (15 mol%), $TMSN_3$ (4.0 eq.), TBPB (5.0 eq.), 70°C.

shown in Figures 1G and 1H, the polymerization is verified by the disappearance of absorption bands at 1,628 and 988,906 cm^{-1}, which were assigned to the stretching vibration of C=C and in-plane bending and wagging vibration of = C-H in the alkene, respectively. Meanwhile, new spectral bands due to carbon-carbon bond formation and carbon-azide bond formation appeared at 1,249 and 2,103 cm^{-1}. These are the stretching vibration of C-F and N_3, respectively. The tiny amount of residual signal from the vinyl group at 6.70, 5.72, and 5.24 ppm and the signal from the iodide at −58.59 ppm (CF_2-I) in ^1H NMR and ^{19}F NMR spectra of the polymer verify the presence of the terminal vinyl group and iodide at each end of the polymer chain. The successful preparation of the polymer is further verified by GPC curve with a M_n of 5,100 and PDI of 1.78. These results of vinyl group addition, carbon-carbon bond formation, carbon-azide bond formation, and terminal groups are all confirmed and are evidence for the successful iron-catalyzed RCP of 1,4-divinylbenzene, 1,4-diiodoperfluorobutane, and $TMSN_3$, resulting in an azide-containing polymer with a terminal vinyl group and an iodide on each end of the polymer chain. Other examples of RCP are listed in Table 1 and Figures S1–S9. These results serve to confirm that these RCPs

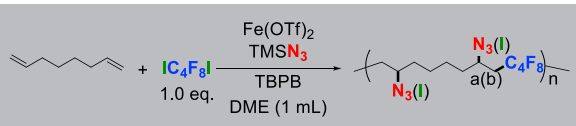

Entry	$TMSN_3$(X eq.)	$Fe(OTf)_2$ (X mol%)	TBPB (X eq.)	Temperature (°C)	N_3/I (a/b)
1	1.0	5	3.0	40	0.97:1
2	1.5	5	3.0	40	2.4:1
3	2.5	5	3.0	r.t	2:1
4	4.0	10	5.0	40	3.0:1
5	4.0	10	5.0	50	3.6:1
6	4.0	15	5.0	70	>49:1

Table 2. Results of the Influence of Feed Ratio and Polymerization Condition on Controlled Azide/Iodine Modification via One-Step RCP

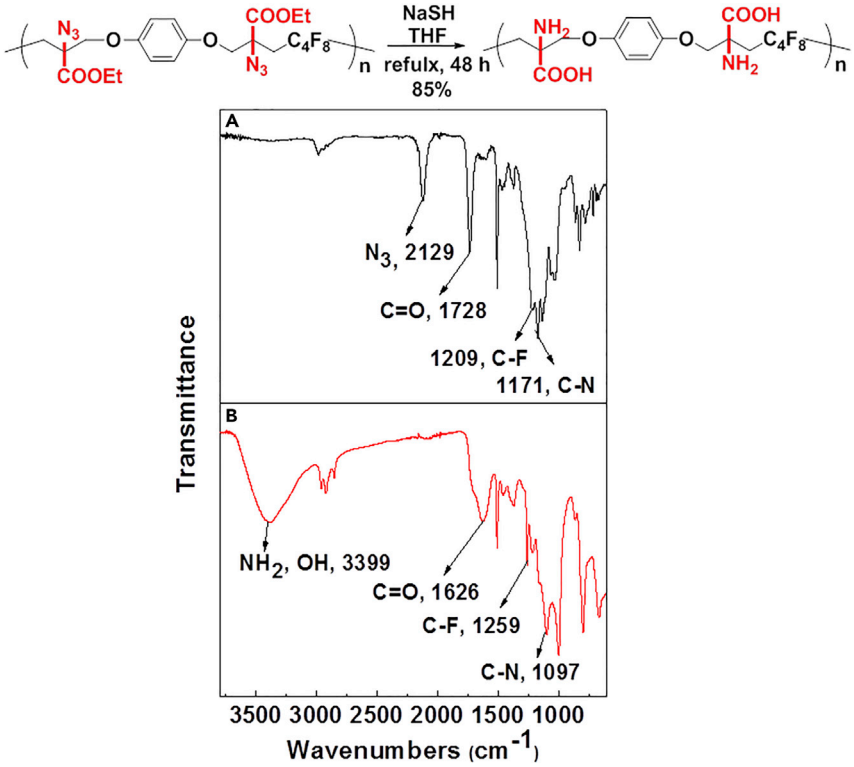

Figure 3. Reduction and Deprotection of Precursor in the Preparation of Poly(α-Amino Acid)

(A) FTIR spectrum of poly(α-amino acid) precursor.

(B) FTIR spectrum of poly(α-amino acid).

undergo vinyl group addition, carbon-carbon bond formation, and carbon-azide bond formation, resulting in polymerization and complete modification in one step.

It is also clear that the introduction of RCR into polymer chemistry works smoothly not only for styrene-like monomers, but also for acrylates and alkyl alkenes, giving polymers with moderate molecular weight and high conversion. These results indicate this developed RCP is a versatile method to enable polymerization and modification in one step. For styrene and acrylate monomers, their RCP gives complete conversion of carbon-azide bond formation, resulting in fully functionalized products. When an alkyl alkene was used as monomer, its RCP exhibited controlled azide/iodine modification of the resulting polymers, as shown in Figure 2 and Figure S10. With the increase in the amount of $TMSN_3$, $Fe(OTf)_2$, and temperature, the azide/iodine ratio can be tuned and increased from 2.4:1 to >49:1. Detailed investigations on the influence of catalyst amount, $TMSN_3$ amount, and temperature on controlled modification are shown in Table 2. As $Fe(OTf)_2$, $TMSN_3$, and temperature are increased, the less stable iodine product will form corresponding radical and transfer to azide product, resulting in the decrease of iodine and the increase of azide. So, the azide/iodine ratio can be adjusted from 0.97/1 to >49:1, correspondingly. Traditional cascade or tandem polymerizations are carried out stepwise or in tandem with different polymerization mechanisms, different reaction types, or different monomers in one pot (Grubbs et al., 1997; Qi et al., 2019; Nakatani et al., 2009; Chen et al., 2006; Kang et al., 2017; Wang et al., 2012). This RCP, however, is realized in a one-step radical procedure through RCR. The introduction of RCR into polymer chemistry in the development of the RCP method is therefore novel in that it offers versatile control of polymerization and modification in one step.

The introduction of RCR into polymer chemistry not only demonstrates versatility in the control of polymerization and modification in one step, but also enables the synthesis of a series of α, β, and γ type poly(amino acid) precursors, as shown in Table 1. Taking the polymer precursor shown in Figure 4 as an example, further reduction of the azide to an amine and deprotection of the ester to a carboxylic acid by NaSH results in polymers containing amino acids. The successful preparation of this α-amino acid containing polymer is

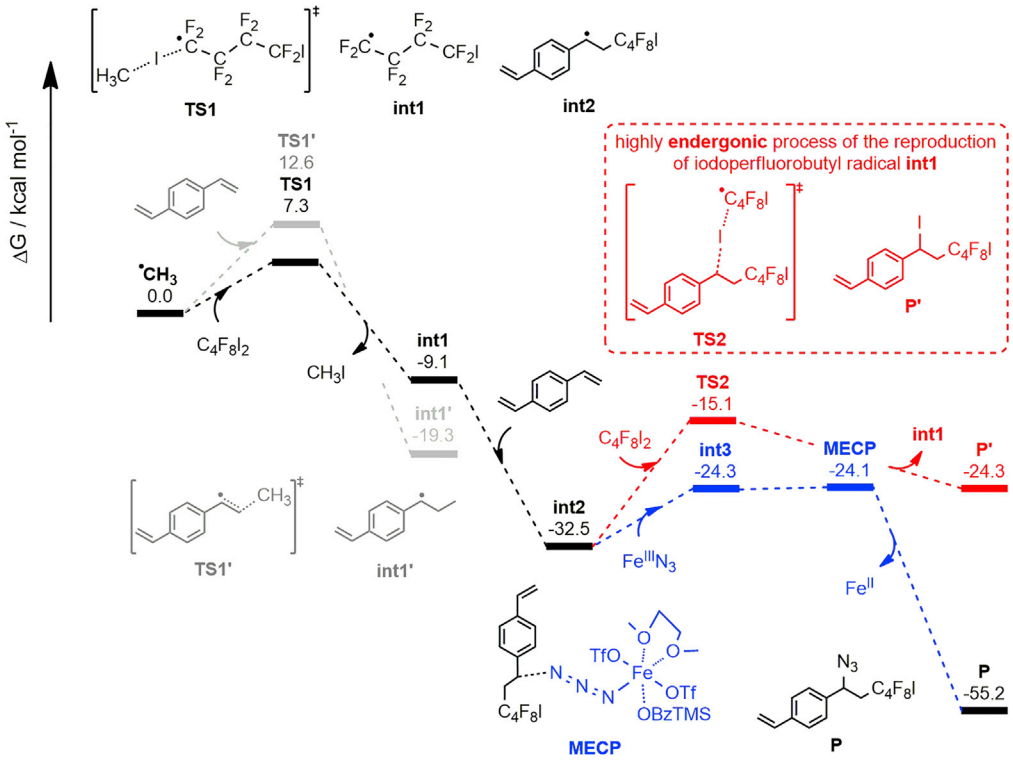

Figure 4. The Free Energy Profile of RCP Involving 1,4-Divinylbenzene

confirmed by FTIR spectra, as shown in Figure 3, which shows the complete disappearance of absorption bands at 2,129 cm^{-1} (stretching vibration of azide group) and the appearance of a new broad signal at 3,399 cm^{-1} from the stretching vibrations of the amine and hydroxide groups. Meanwhile, the stretching vibration of C=O was shifted from 1,728 to 1,626 cm^{-1} owing to the conversion of ester groups to carboxylic acid groups. These azide-containing polymers show other potential applications with regards to the versatile azide group. An example of this is the production of bottlebrush polymers.

Mechanistic Study

To further investigate the mechanism of RCP, density functional theory studies were also conducted to exhibit how RCP realizes synchronized polymerization and modification in one cascaded step. The results for RCR of 1,4-divinylbenzene or octa-1,7-diene, 1,4-diiodoperfluorobutane and $TMSN_3$ are shown in Figures 4 and S11, respectively. Once the carbon radical is formed through a single electron transfer from the iron (II) catalyst to TBPB, the iodine abstraction between 1,4-diiodoperfluorobutane and the formed carbon radical in the formation of an iodoperfluorobutyl radical (int1) shows the lowest barrier pathway with only 7.3 kcal/mol of free energy barrier. Then, the perfluorobutyl radical adds onto the 1,4-divinylbenzene without barrier to deliver the benzyl radical int2 with high exergonicity of 32.5 kcal/mol. These free energy-favored processes guarantee the efficiency and selectivity of carbon-carbon bond formation in the formation of int2 to inhibit the radical polymerization of alkene by itself. Further calculations indicate **int2** will undergo two competitive pathways through reacting with a $C_4F_8I_2$ or a $Fe^{III}N_3$ depending on alkene types, resulting in formation of carbon-azide bond and carbon-iodine bond, respectively. For styrene-type monomer, it shows sufficient efficiency and selectivity on the carbon-azide bond formation, attributed to the unfavorable iodoperfluorobutyl radical reproduction by the stable benzyl radical int2, which is an endergonic pathway with relatively higher barrier of 17.4 kcal/mol (Figure 4). For alkyl alkene-type monomer, the observation of iodine addition product in the reaction of octa-1,7-diene is due to the homenergic iodoperfluorobutyl radical reproduction by alkyl radical int4 with lower barrier (14.5 kcal/mol, Figure S11), resulting in tunable carbon-azide bond and carbon-iodine bond formations by adjusting the amount of $TMSN_3$ and $Fe(OTf)_2$.

Based on the above characterizations of polymer structures and mechanism studies, a plausible mechanism for this iron-catalyzed three-component alkene carboazidation RCP is shown in Scheme 2. This RCP

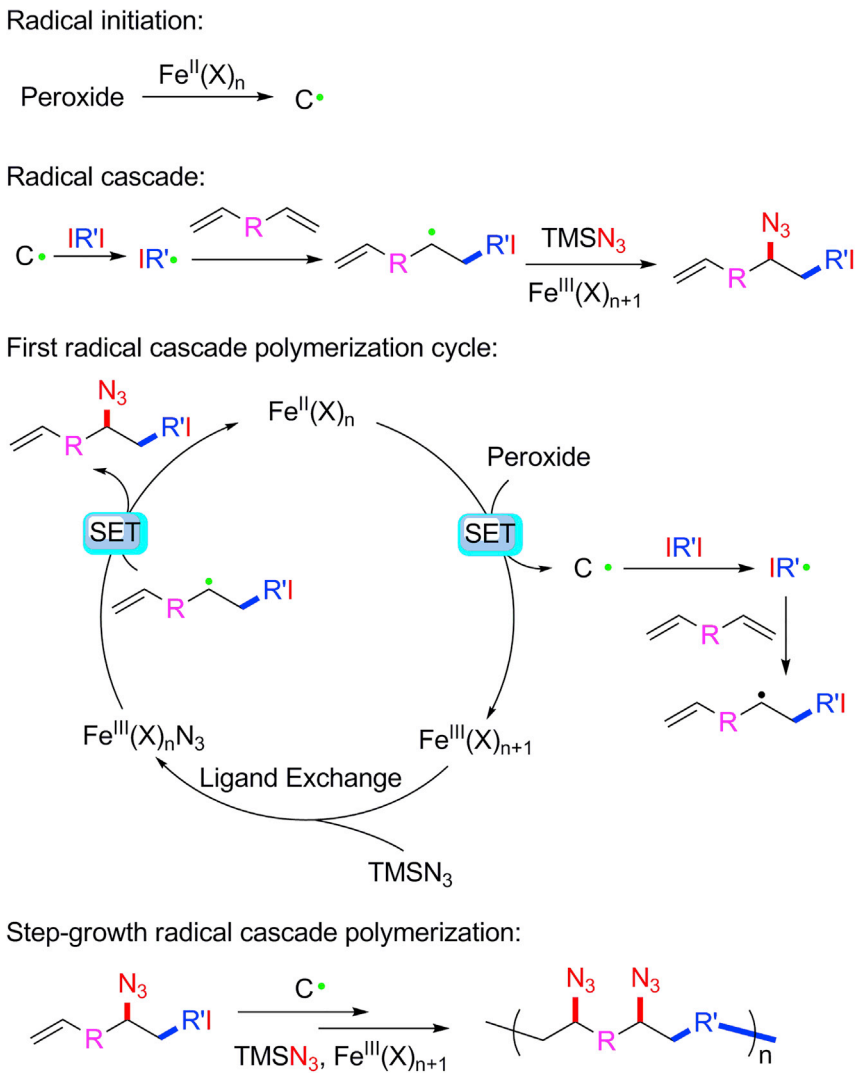

Scheme 2. Mechanism of Iron-Catalyzed Three-Component Alkene Carboazidation RCP Through Alkene Functionalization Polymerization

is initiated by a single electron transfer from the iron (II) catalyst to TBPB generating a carbon radical (C•) and an iron (III) complex. The iodine atom in the diiodo compound was abstracted by the carbon radical to form a new radical (IR'•), which will add to the divinyl alkene giving an intermediate. Meanwhile, the iron (III) complex exchanges the ligand with $TMSN_3$ to generate the iron (III) azide complex, which reacts with a radical intermediate to end one radical cascade polymerization cycle with the formation of an azide-containing iodoalkene compound and iron (II) complex which is used in the next polymerization cycle. With the continuous step-growth RCR, the iron-catalyzed three-component alkene carboazidation type of RCR has been successfully introduced to polymer chemistry in the development of RCP, enabling synchronized polymerization and modification in one pot, where the sufficient efficiency and selectivity on the carbon-carbon bond and carbon-azide bond formations play key roles.

Conclusion

In summary, we have successfully introduced the radical cascade reaction into polymer chemistry. This has resulted in the development of radical cascade polymerization toward synchronized polymerization and modification in one pot. In this process, the high efficiency and selectivity of iron-catalyzed three-component alkene carboazidation on the carbon-carbon and carbon-azide bond formation play significant and critical roles in alkene functionalization polymerization. Through iron-catalyzed three-component alkene

carboazidation radical cascade polymerization, a series of azide-containing functional polymers have been prepared, including a series of α, β, and γ poly(amino acid) precursors. This work therefore expands the methodology library of polymerization and provides a one-step strategy for synchronized polymerization and modification. In view of the rapid development in radical cascade reactions of alkene difunctionalization in the last 10 years and the ever-increasing research interests on this area in organic chemistry, this work also opens up a window for polymer science to achieve functional polymers with tailored chemical functionality not limited to azide during *in situ* polymerization.

Limitations of the Study

This study focuses on the demonstration of synchronized polymerization and modification in one step, by introducing radical cascade reaction into polymer chemistry to develop a new polymerization methodology, i.e., radical cascade polymerization. The substrates used in this study contain perfluorobutanes, which may cause difficulty in investigating the functionalities of resulting poly(amino acid)s in aqueous solution. Fortunately, the solubility deriving from the substrates will form hydrophobic domain of poly(amino acid)s and endow poly(amino acid)s with amphiphilicity, which may exhibit special functionality as self-assemblies in aqueous solution.

METHODS

All methods can be found in the accompanying Transparent Methods supplemental file.

SUPPLEMENTAL INFORMATION

Supplemental Information can be found online at https://doi.org/10.1016/j.isci.2020.100902.

ACKNOWLEDGMENTS

We thank the NSFC (21922112, 21971236, 21672213, and 21871258), the National Key R&D Program of China (2017YFA0700103), the Strategic Priority Research Program of the Chinese Academy of Sciences (XDB20000000), and the Haixi Institute of CAS (CXZX-2017-P01) for financial support.

AUTHOR CONTRIBUTIONS

H.B. and W.-M.W. directed the investigations and prepared the manuscript. N.Z., M.-F.C., and Y.L. contributed to the discussion and preparation of the manuscript. N.Z., H.X., Min Su, and Muqiao Su performed the experiments and analyzed the experimental data. M.-F.C. worked on the theoretical calculations.

DECLARATION OF INTERESTS

The authors declare no competing interests.

Received: October 14, 2019
Revised: December 10, 2019
Accepted: December 20, 2019
Published: March 27, 2020

REFERENCES

Baggett, A.W., Guo, F., Li, B., Liu, S.Y., and Jäkle, F. (2015). Regioregular synthesis of azaborine oligomers and a polymer with a syn conformation stabilized by NH•••π interactions. Angew. Chem. Int. Ed. *54*, 11191–11195.

Bao, Z., Chan, W.K., and Yu, L. (1995). Exploration of the Stille coupling reaction for the synthesis of functional polymers. J. Am. Chem. Soc. *117*, 12426–12435.

Bielawski, C.W., and Grubbs, R.H. (2000). Highly efficient ring-opening metathesis polymerization (ROMP) using new ruthenium catalysts containing N-Heterocyclic carbene ligands. Angew. Chem. Int. Ed. *39*, 2903–2906.

Bielawski, C.W., and Grubbs, R.H. (2007). Living ring-opening metathesis polymerization. Prog. Polym. Sci. *32*, 1–29.

Boaen, N.K., and Hillmyer, M.A. (2005). Post-polymerization functionalization of polyolefins. Chem. Soc. Rev. *34*, 267–275.

Brill, Z.G., Grover, H.K., and Maimone, T.J. (2016). Enantioselective synthesis of an ophiobolin sesterterpene via a programmed radical cascade. Science *352*, 1078–1082.

Britovsek, G.J.P., Gibson, V.C., and Wass, D.F. (1999). The search for new-generation olefin polymerization catalysts: life beyond metallocenes. Angew. Chem. Int. Ed. *38*, 428–447.

Chen, G.H., Huynh, D., Felgner, P.L., and Guan, Z.B. (2006). Tandem chain walking polymerization and atom transfer radical polymerization for efficient synthesis of dendritic nanoparticles for bioconjugation. J. Am. Chem. Soc. *128*, 4298–4302.

Chiefari, J., Chong, Y.K., Ercole, F., Krstina, J., Jeffery, J., Le, T.P.T., Mayadunne, R.T.A., Meijs, G.F., Moad, C.L., Moad, G., et al. (1998). Living free-radical polymerization by reversible Addition−Fragmentation chain Transfer: the RAFT process. Macromolecules *31*, 5559–5562.

Deng, H.Q., Han, T., Zhao, E.G., Kwok, R.T.K., Lam, J.W.Y., and Tang, B.Z. (2016). Multicomponent click polymerization: a facile strategy toward fused heterocyclic polymers. Macromolecules *49*, 5475–5483.

Deng, X.X., Li, L., Li, Z.L., Lv, A., Du, F.S., and Li, Z.C. (2012). Sequence regulated poly(ester-amide)s based on passerini reaction. ACS Macro Lett. *1*, 1300–1303.

Gao, Y., Wang, X., Tong, L., Qin, A.J., Sun, J.Z., and Tang, B.Z. (2014). A new strategy of post-polymerization modification to prepare functionalized poly(disubstituted acetylenes). Polym. Chem. *5*, 2309–2319.

Gauthier, M.A., Gibson, M.I., and Klok, H.A. (2009). Synthesis of functional polymers by post-polymerization modification. Angew. Chem. Int. Ed. *48*, 48–58.

Grubbs, R.B., Hawker, C.J., Dao, J., and Fréchet, J.M.J. (1997). A tandem approach to graft and dendritic graft copolymers based on 'living' free radical polymerizations. Angew. Chem. Int. Ed. *36*, 270–272.

Guo, F., Yin, X., Pammer, F., Cheng, F., Fernandez, D., Lalancette, R.A., and Jäkle, F. (2014). Regioregular organoborane-functionalized poly(3-alkynylthiophene)s. Macromolecules *47*, 7831–7841.

He, B.Z., Su, H.F., Bai, T.W., Wu, Y.W., Li, S.W., Gao, M., Hu, R.R., Zhao, Z.J., Qin, A.J., Ling, J., and Tang, B.Z. (2017). Spontaneous amino-yne click polymerization: a powerful tool toward regio- and stereospecific poly(beta-aminoacrylate)s. J. Am. Chem. Soc. *139*, 5437–5443.

He, B.Z., Zhen, S.J., Wu, Y.W., Hu, R.R., Zhao, Z.J., Qin, A.J., and Tang, B.Z. (2016). Cu(I)-Catalyzed amino-yne click polymerization. Polym. Chem. *7*, 7375–7382.

Hedir, G.G., Bell, C.A., O'reilly, R.K., and Dove, A.P. (2015). Functional degradable polymers by radical ring-opening copolymerization of MDO and vinyl bromobutanoate: synthesis, degradability and post-polymerization modification. Biomacromolecules *16*, 2049–2058.

Huang, H., Wang, W., Zhou, Z., Sun, B., An, M., Haeffner, F., and Niu, J. (2019). Radical ring-closing/ring-opening cascade polymerization. J. Am. Chem. Soc. *141*, 12493–12497.

Jiang, K.M., Zhang, L., Zhao, Y.C., Lin, J., and Chen, M. (2018). Palladium-catalyzed cross-coupling polymerization: a new access to cross-conjugated polymers with modifiable structure and tunable optical/conductive properties. Macromolecules *51*, 9662–9668.

Jing, Y.-N., Li, S.-S., Su, M., Bao, H., and Wan, W.-M. (2019). Barbier Hyperbranching polymerization-induced emission toward facile fabrication of white light-emitting diode and light-harvesting film. J. Am. Chem. Soc. *141*, 16839–16848.

Kakuchi, R., and Theato, P. (2013). Three-component reactions for post-polymerization modifications. ACS Macro Lett. *2*, 419–422.

Kamigaito, M., Ando, T., and Sawamoto, M. (2001). Metal-catalyzed living radical polymerization. Chem. Rev. *101*, 3689–3745.

Kang, C., Park, H., Lee, J.K., and Choi, T.L. (2017). Cascade polymerization via controlled tandem olefin metathesis/metallotropic 1,3-shift reactions for the synthesis of fully conjugated polyenynes. J. Am. Chem. Soc. *139*, 11309–11312.

Kotha, S., Lahiri, K., and Kashinath, D. (2002). Recent applications of the Suzuki–Miyaura cross-coupling reaction in organic synthesis. Tetrahedron *58*, 9633–9695.

Kreye, O., Toth, T., and Meier, M.A.R. (2011). Introducing multicomponent reactions to polymer science: passerini reactions of renewable monomers. J. Am. Chem. Soc. *133*, 1790–1792.

Littke, A.F., Dai, C., and Fu, G.C. (2000). Versatile catalysts for the Suzuki cross-coupling of arylboronic acids with aryl and vinyl halides and triflates under mild conditions. J. Am. Chem. Soc. *122*, 4020–4028.

Littke, A.F., and Fu, G.C. (1999). The first general method for Stille cross-couplings of aryl chlorides. Angew. Chem. Int. Ed. *38*, 2411–2413.

Liu, M., Vladimirov, N., and Fréchet, J.M.J. (1999). A new approach to Hyperbranched polymers by ring-opening polymerization of an AB monomer: 4-(2-Hydroxyethyl)-ϵ-caprolactone. Macromolecules *32*, 6881–6884.

Liu, Y., Wu, D.C., Ma, Y.X., Tang, G.P., Wang, S., He, C.B., Chung, T.S., and Goh, S. (2003). Novel poly(amino ester)s obtained from Michael addition polymerizations of trifunctional amine monomers with diacrylates: safe and efficient DNA carriers. Chem. Commun. (Camb.), 2630–2631.

Lv, X.H., Li, S.S., Tian, C.Y., Yang, M.M., Li, C., Zhou, Y., Sun, X.L., Zhang, J., and Wan, W.M. (2017). Borinic acid polymer: simplified synthesis and enzymatic biofuel cell application. Macromol. Rapid Commun. *38*, 1600687.

Matyjaszewski, K., and Xia, J.H. (2001). Atom transfer radical polymerization. Chem. Rev. *101*, 2921–2990.

Miyaura, N., Yanagi, T., and Suzuki, A. (1981). The palladium-catalyzed cross-coupling reaction of phenylboronic acid with haloarenes in the presence of bases. Synth. Commun. *11*, 513–519.

Moad, G., Rizzardo, E., and Thang, S.H. (2005). Living radical polymerization by the RAFT process. Aust. J. Chem. *58*, 379–410.

Moad, G., Rizzardo, E., and Thang, S.H. (2008). Radical addition–fragmentation chemistry in polymer synthesis. Polymer *49*, 1079–1131.

Nakatani, K., Terashima, T., and Sawamoto, M. (2009). Concurrent tandem living radical polymerization: gradient copolymers via in situ monomer transformation with alcohols. J. Am. Chem. Soc. *131*, 13600–13601.

Pintauer, T., and Matyjaszewski, K. (2008). Atom transfer radical addition and polymerization reactions catalyzed by ppm amounts of copper complexes. Chem. Soc. Rev. *37*, 1087–1097.

Plesniak, M.P., Huang, H.M., and Procter, D.J. (2017). Radical cascade reactions triggered by single electron transfer. Nat. Rev. Chem. *1*, 0077.

Qi, C.X., Zheng, C., Hu, R.R., and Tang, B.Z. (2019). Direct construction of acid-responsive poly(indolone)s through multicomponent tandem polymerizations. ACS Macro Lett. *8*, 569–575.

Richards, S.J., Jones, M.W., Hunaban, M., Haddleton, D.M., and Gibson, M.I. (2012). Probing bacterial-toxin inhibition with synthetic glycopolymers prepared by tandem post-polymerization modification: role of linker length and carbohydrate density. Angew. Chem. Int. Ed. *51*, 7812–7816.

Schluter, A.D. (2001). The tenth anniversary of Suzuki polycondensation (SPC). J. Polym. Sci. A Polym. Chem. *39*, 1533–1556.

Sun, J.T., Hong, C.Y., and Pan, C.Y. (2013). Recent advances in RAFT dispersion polymerization for preparation of block copolymer aggregates. Polym. Chem. *4*, 873–881.

Sun, X.L., Liu, D.M., Tian, D., Zhang, X.Y., Wu, W., and Wan, W.M. (2017). The introduction of the Barbier reaction into polymer chemistry. Nat. Commun. *8*, 1210.

Tebben, L., and Studer, A. (2011). Nitroxides: applications in synthesis and in polymer chemistry. Angew. Chem. Int. Ed. *50*, 5034–5068.

Vougioukalakis, G.C., and Grubbs, R.H. (2010). Ruthenium-Based heterocyclic carbene-coordinated olefin metathesis catalysts. Chem. Rev. *110*, 1746–1787.

Wan, W.M., Cheng, F., and Jäkle, F. (2014). A borinic acid polymer with fluoride ion- and thermo-responsive properties that are tunable over a wide temperature range. Angew. Chem. Int. Ed. *53*, 8934–8938.

Wan, W.M., Li, S.S., Liu, D.M., Lv, X.H., and Sun, X.L. (2017). Synthesis of electron-deficient borinic acid polymers with multiresponsive properties and their application in the fluorescence detection of alizarin red S and electron-rich 8-Hydroxyquinoline and fluoride ion: substituent effects. Macromolecules *50*, 6872–6879.

Wang, D., Liu, Y., Hu, Z.C., Hong, C.Y., and Pan, C.Y. (2005). Michael addition polymerizations of trifunctional amines with diacrylamides. Polymer *46*, 3507–3514.

Wang, F., Chen, P.H., and Liu, G.S. (2018). Copper-catalyzed radical relay for asymmetric radical transformations. Acc. Chem. Res. *51*, 2036–2046.

Wang, J.S., and Matyjaszewski, K. (1995). Controlled/"living" radical polymerization. atom transfer radical polymerization in the presence of transition-metal complexes. J. Am. Chem. Soc. *117*, 5614–5615.

Wang, S.Q., Fu, C.K., Zhang, Y., Tao, L., Li, S.X., and Wei, Y. (2012). One-pot cascade synthetic strategy: a smart combination of chemoenzymatic transesterification and raft polymerization. ACS Macro Lett. *1*, 1224–1227.

Wang, X., Xia, D., Qin, W., Zhou, R., Zhou, X., Zhou, Q., Liu, W., Dai, X., Wang, H., Wang, S.,

et al. (2017a). A radical cascade enabling collective syntheses of natural products. Chem *2*, 803–816.

Wang, Z.L., Yu, Y., Li, Y.S., Yang, L., Zhao, Y., Liu, G.Q., Wei, Y., Wang, X., and Tao, L. (2017b). Post-polymerization modification via the Biginelli reaction to prepare water-soluble polymer adhesives. Polym. Chem. *8*, 5490–5495.

Wei, B., Li, W.Z., Zhao, Z.J., Qin, A.J., Hu, R.R., and Tang, B.Z. (2017). Metal-free multicomponent tandem polymerizations of alkynes, amines, and formaldehyde toward structure- and sequence-controlled luminescent polyheterocycles. J. Am. Chem. Soc. *139*, 5075–5084.

Wu, H.B., Wang, Z.M., and Tao, L. (2017). The Hantzsch reaction in polymer chemistry: synthesis and tentative application. Polym. Chem. *8*, 7290–7296.

Xiong, H.G., Ramkumar, N., Chiou, M.F., Jian, W.J., Li, Y.J., Su, J.H., Zhang, X.H., and Bao, H.L. (2019). Iron-catalyzed carboazidation of alkenes and alkynes. Nat. Commun. *10*, 122.

Xue, H.D., Zhao, Y., Wu, H.B., Wang, Z.L., Yang, B., Wei, Y., Wang, Z.M., and Tao, L. (2016). Multicomponent combinatorial polymerization via the biginelli reaction. J. Am. Chem. Soc. *138*, 8690–8693.

Yin, X., Guo, F., Lalancette, R.A., and Jäkle, F. (2016). Luminescent main-chain organoborane polymers: highly robust, electron-deficient poly(oligothiophene borane)s via Stille coupling polymerization. Macromolecules *49*, 537–546.

Yokoyama, A., Suzuki, H., Kubota, Y., Ohuchi, K., Higashimura, H., and Yokozawa, T. (2007). Chain-growth polymerization for the synthesis of polyfluorene via Suzuki-Miyaura coupling reaction from an externally added initiator unit. J. Am. Chem. Soc. *129*, 7236–7237.

Yu, X.Y., Chen, J.R., Wang, P.Z., Yang, M.N., Liang, D., and Xiao, W.J. (2018). A visible-light-driven iminyl radical-mediated C-C single bond cleavage/radical addition cascade of oxime esters. Angew. Chem.Int. Ed. *57*, 738–743.

Zhang, B., and Studer, A. (2015). Recent advances in the synthesis of nitrogen heterocycles via radical cascade reactions using isonitriles as radical acceptors. Chem. Soc. Rev. *44*, 3505–3521.

iScience, Volume *23*

Supplemental Information

The Introduction of the Radical Cascade Reaction into Polymer Chemistry: A One-Step Strategy for Synchronized Polymerization and Modification

Nengbo Zhu, Mong-Feng Chiou, Haigen Xiong, Min Su, Muqiao Su, Yajun Li, Wen-Ming Wan, and Hongli Bao

Supplemental Figures

NMR Spectra of raw materials

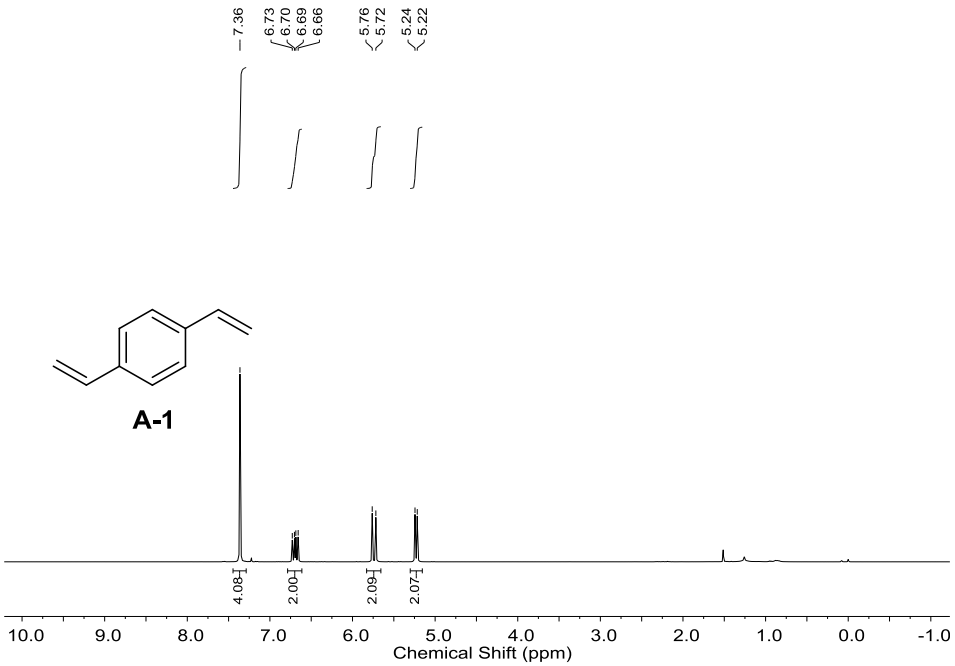

Figure S1: ^{1}H NMR spectrum of compound **A-1,** related to **Table 1.**

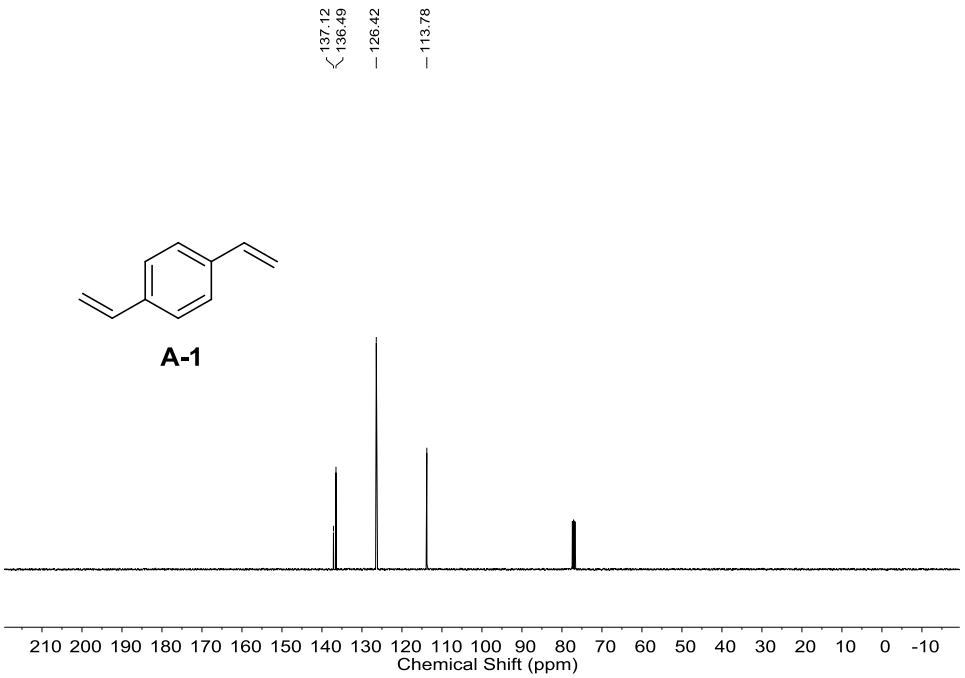

Figure S2: ^{13}C NMR spectrum of compound **A-1,** related to **Table 1.**

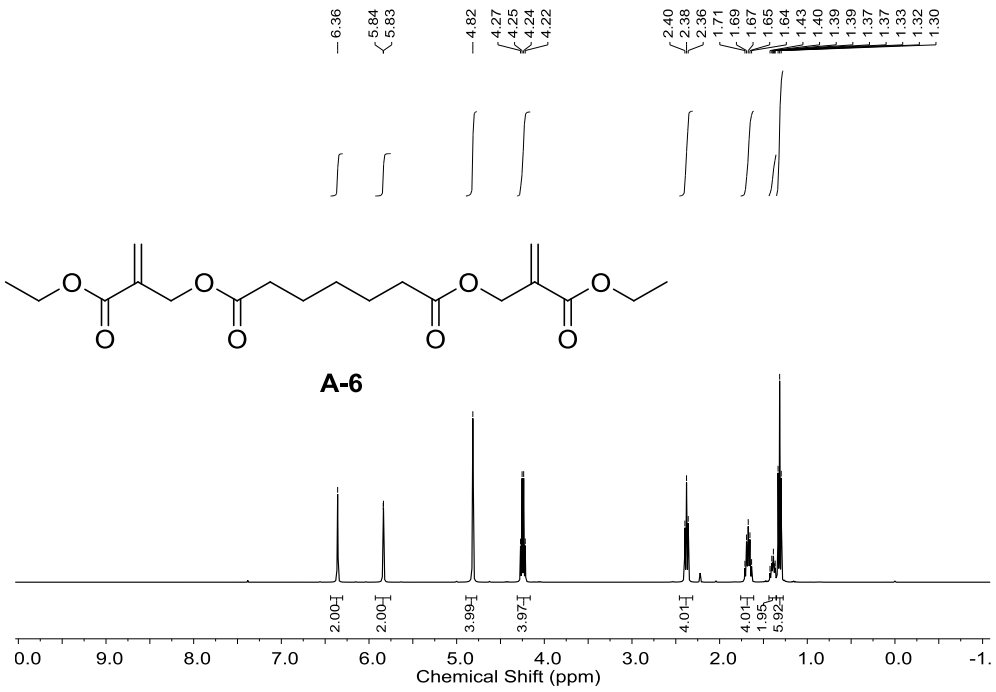

Figure S3: ^{1}H NMR spectrum of compound **A-6,** related to **Table 1.**

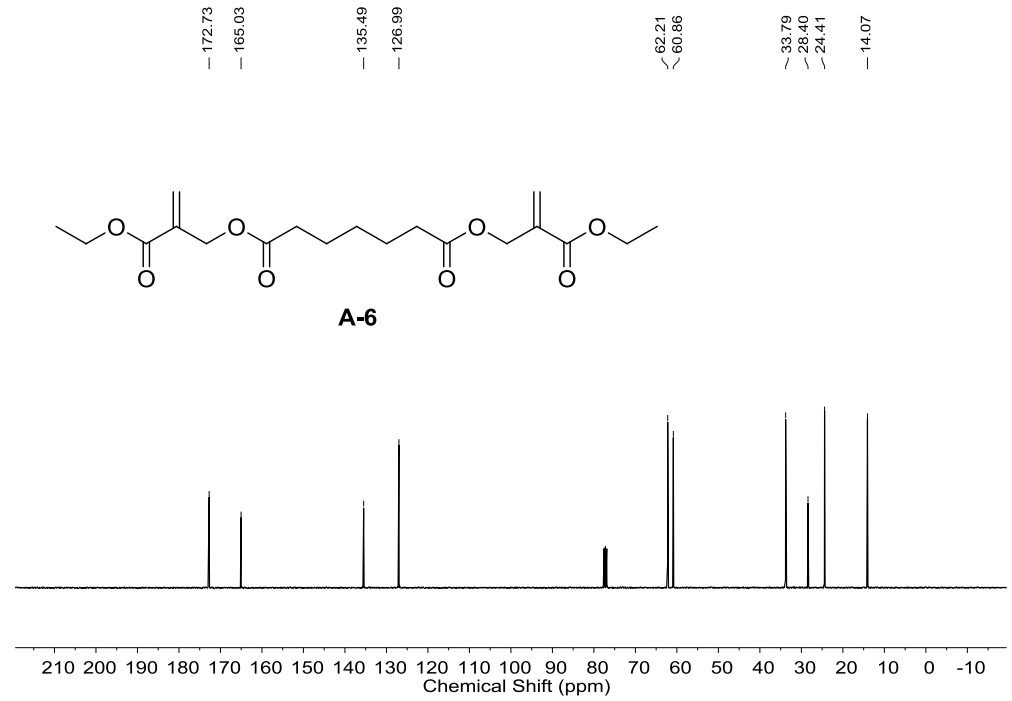

Figure S4: ^{13}C NMR spectrum of compound **A-6,** related to **Table 1.**

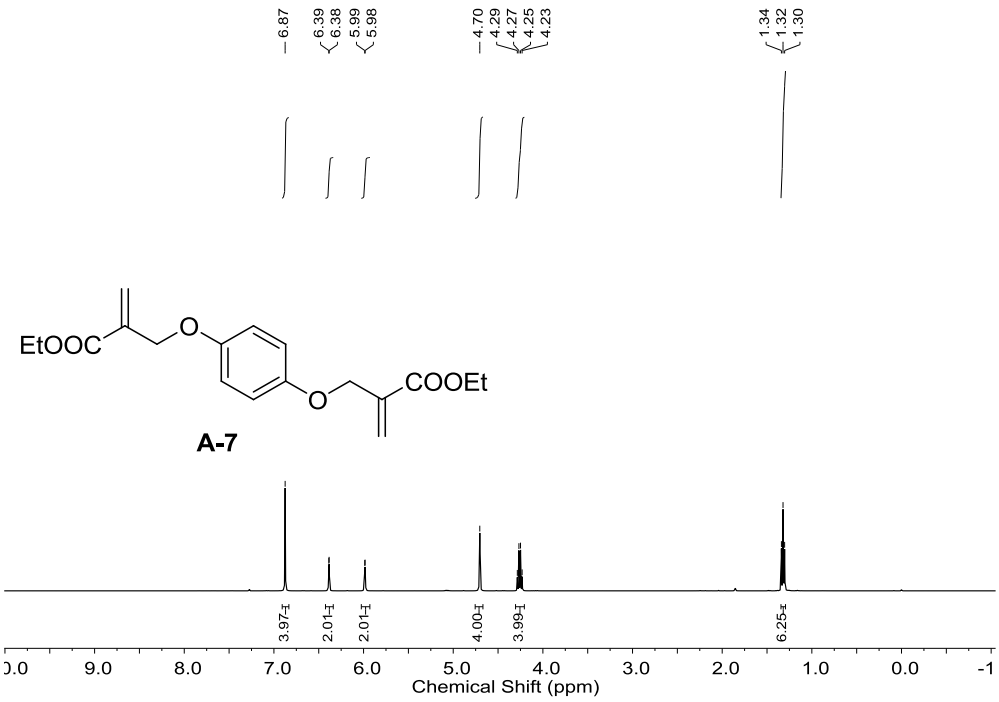

Figure S5: ^{1}H NMR spectrum of compound **A-7,** related to **Table 1.**

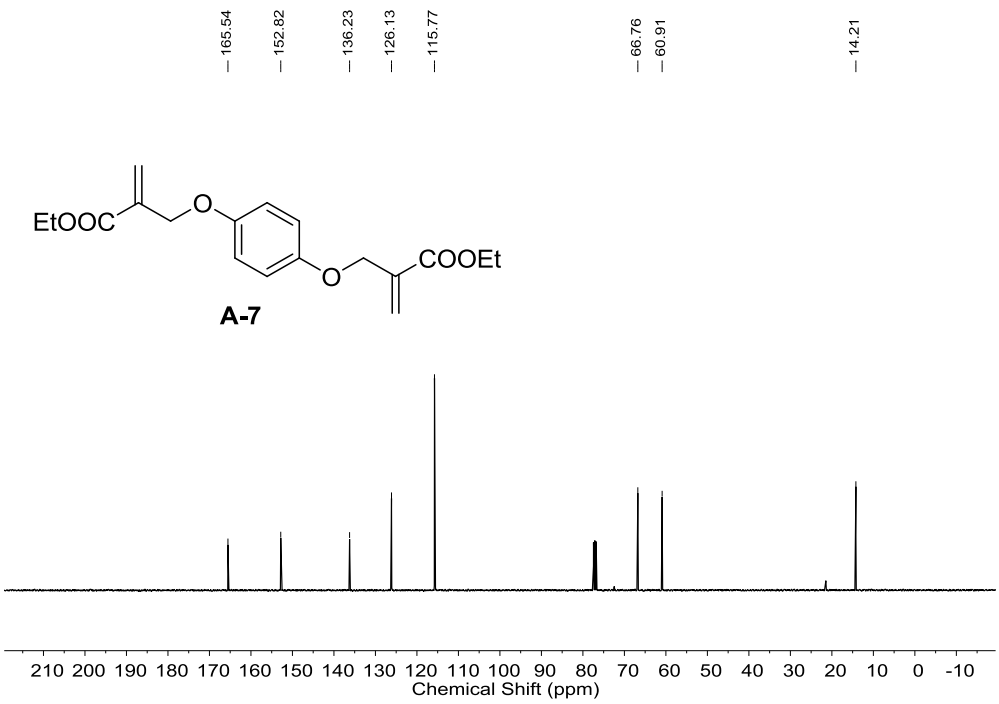

Figure S6: ^{13}C NMR spectrum of compound **A-7,** related to **Table 1.**

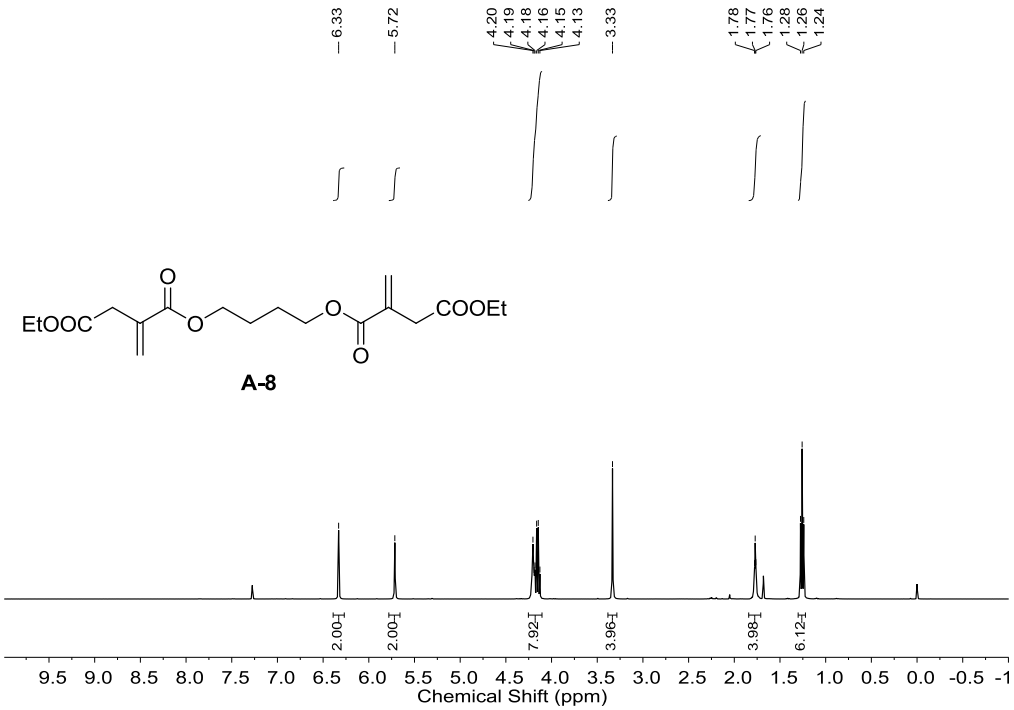

Figure S7: ^{1}H NMR spectrum of compound **A-8,** related to **Table 1.**

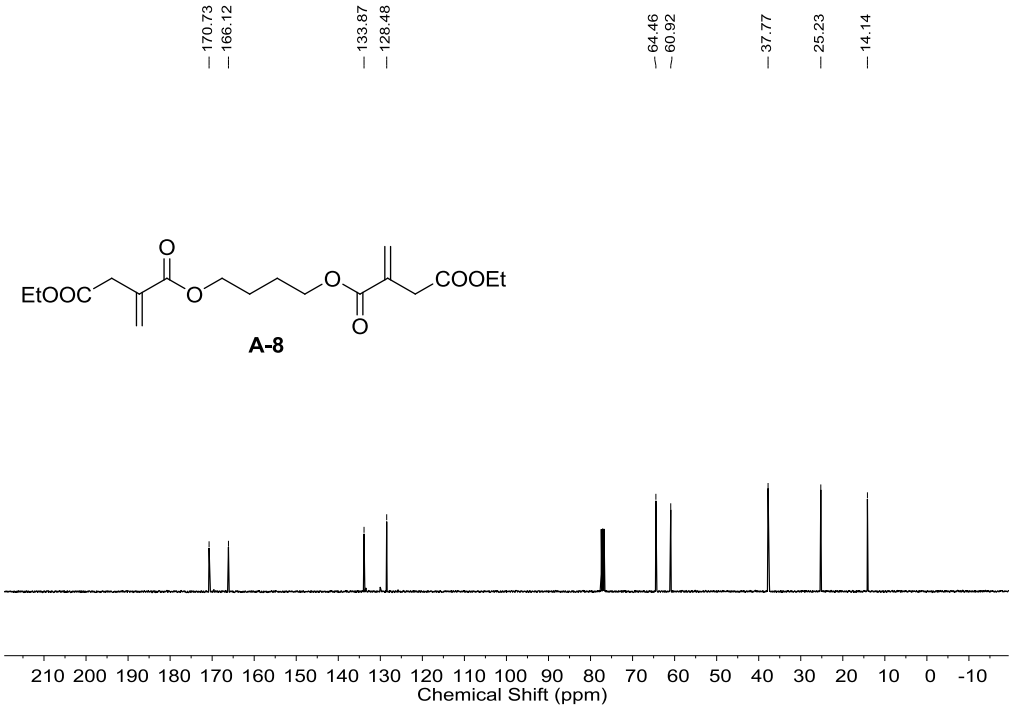

Figure S8: ^{13}C NMR spectrum of compound **A-8,** related to **Table 1.**

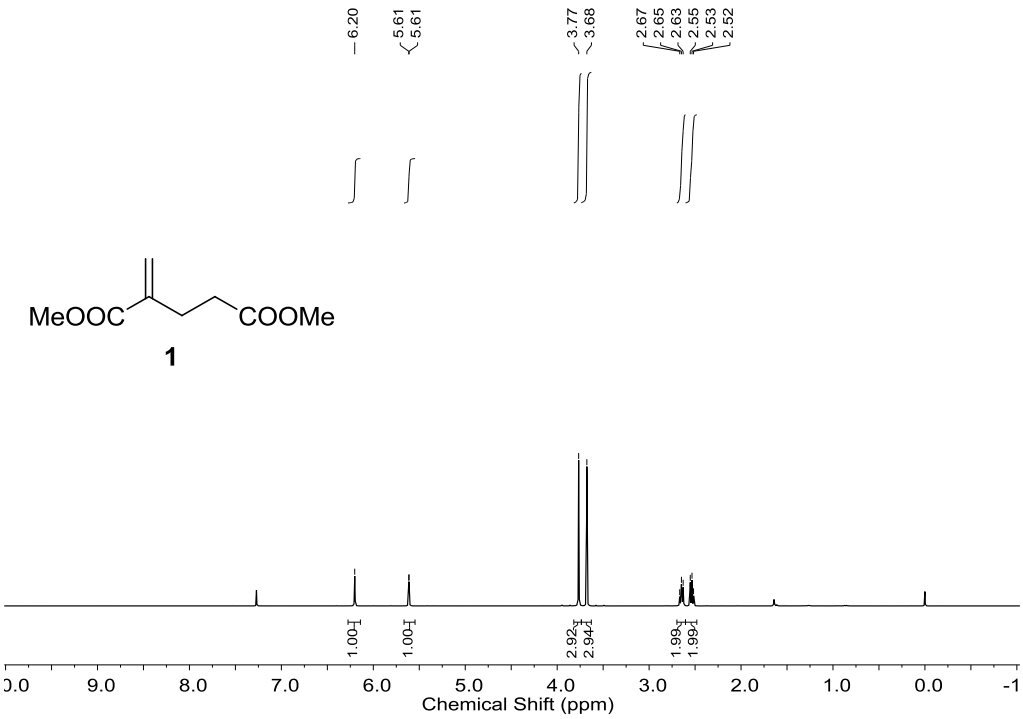

Figure S9: ^{1}H NMR spectrum of compound **1,** related to **Table 1.**

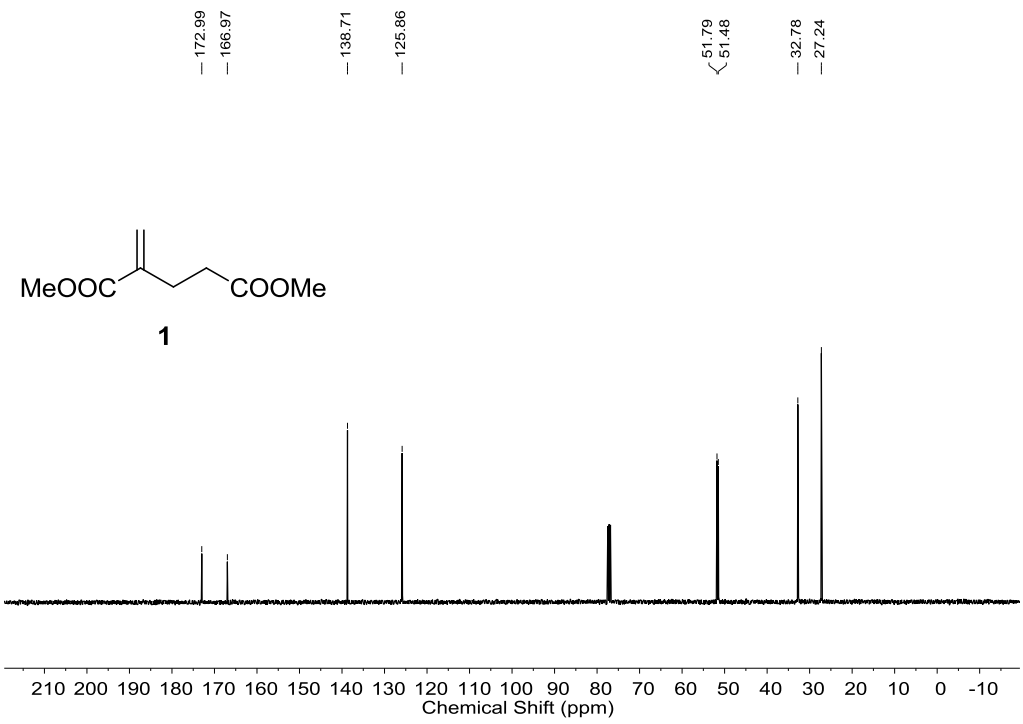

Figure S10: ^{13}C NMR spectrum of compound **1,** related to **Table 1.**

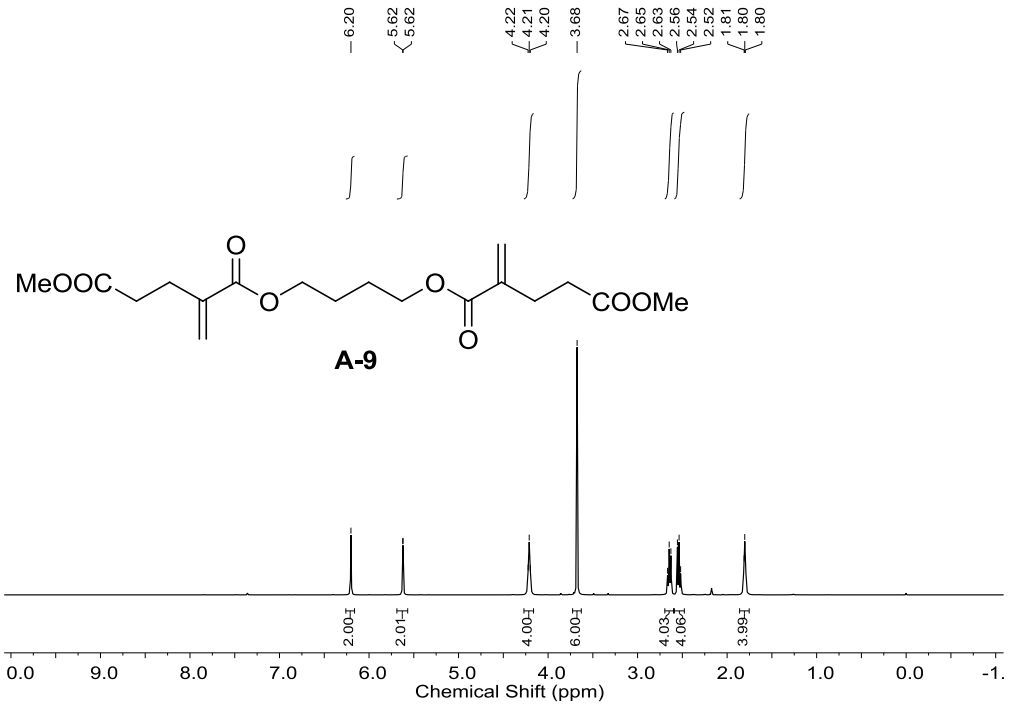

Figure S11: ^{1}H NMR spectrum of compound **A-9,** related to **Table 1.**

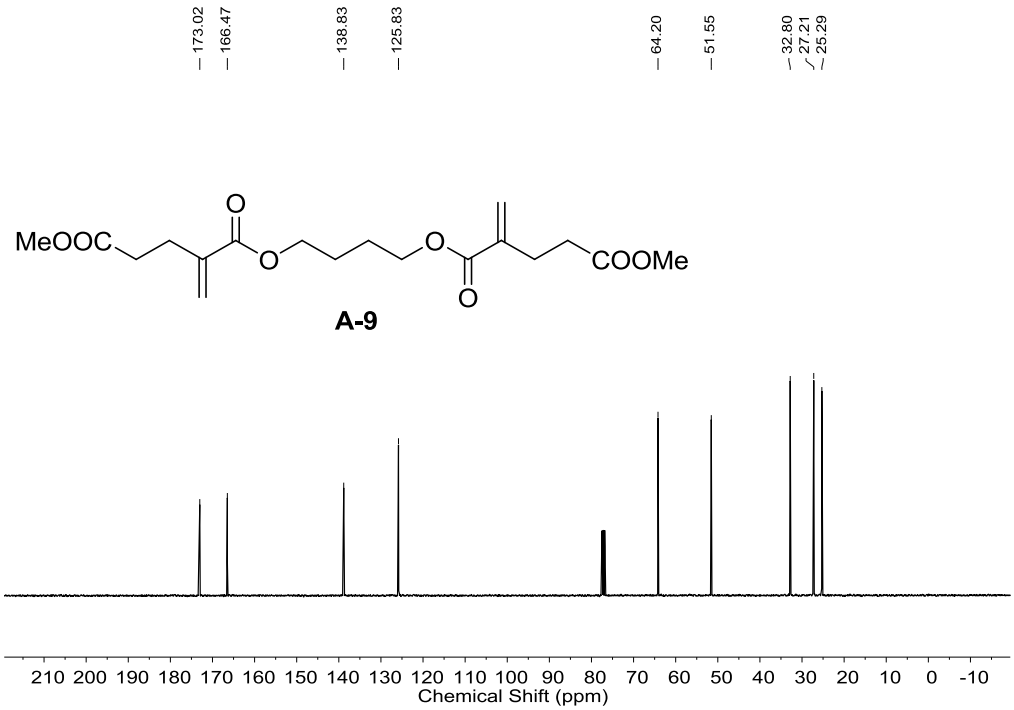

Figure S12: ^{13}C NMR spectrum of compound **A-9,** related to **Table 1.**

Characterization of polymers

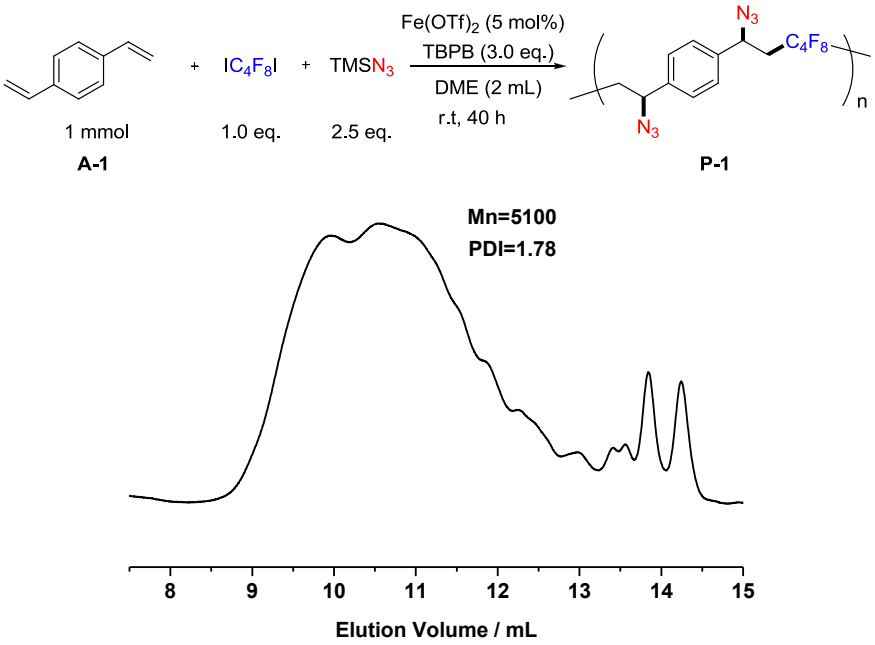

Figure S13: GPC curve of **P-1**, related to **Table 1.**

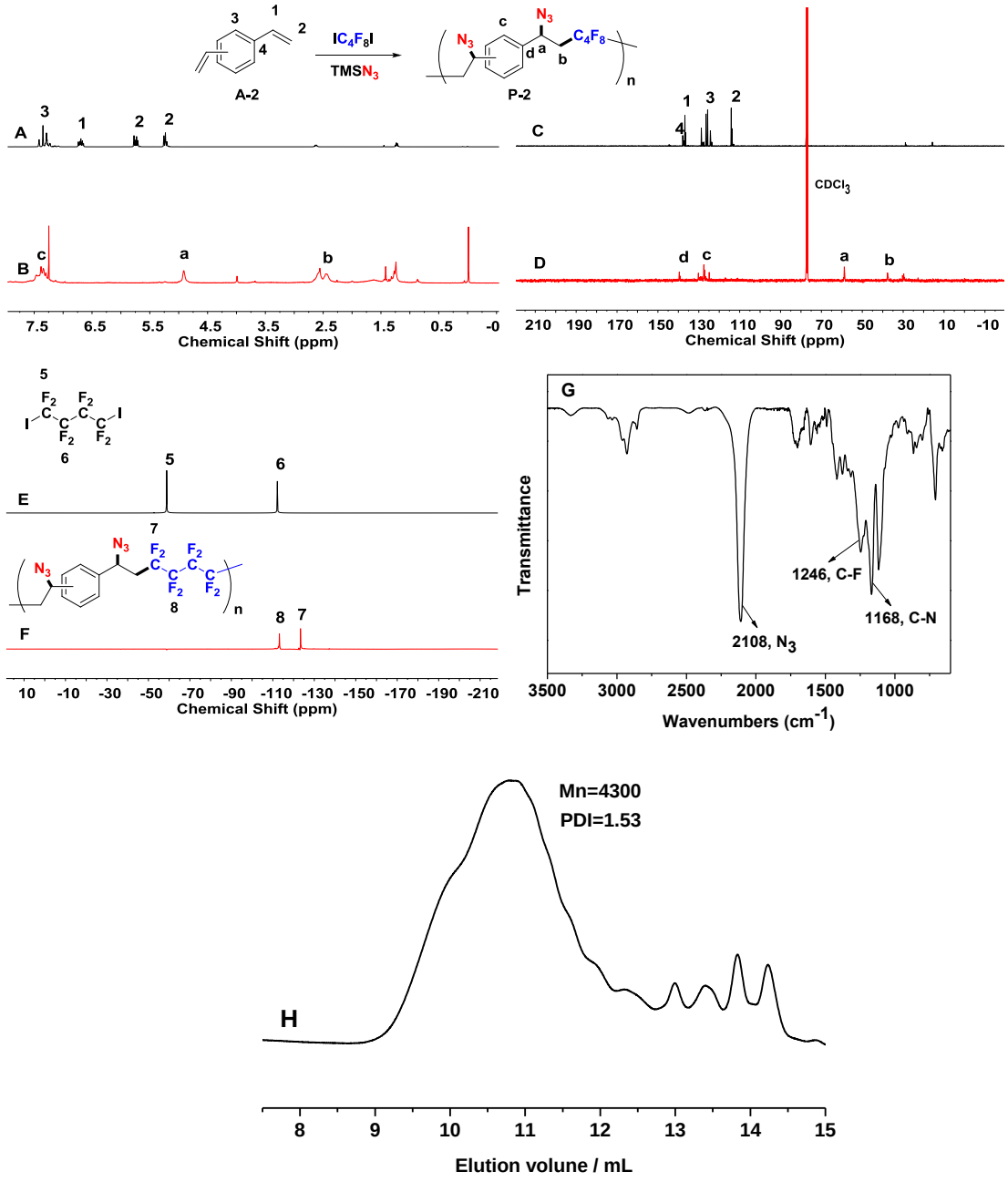

Figure S14: ^{1}H NMR spectra (A: **A-2**; B: **P-2**); ^{13}C NMR spectra (C: **A-2**; D: **P-2**); ^{19}F NMR spectra (E: 1,4-diiodoperfluorobutane; F: **P-2**); FT-IR spectrum of **P-2** (G). GPC curve of **P-2** (H), related to **Table 1.**

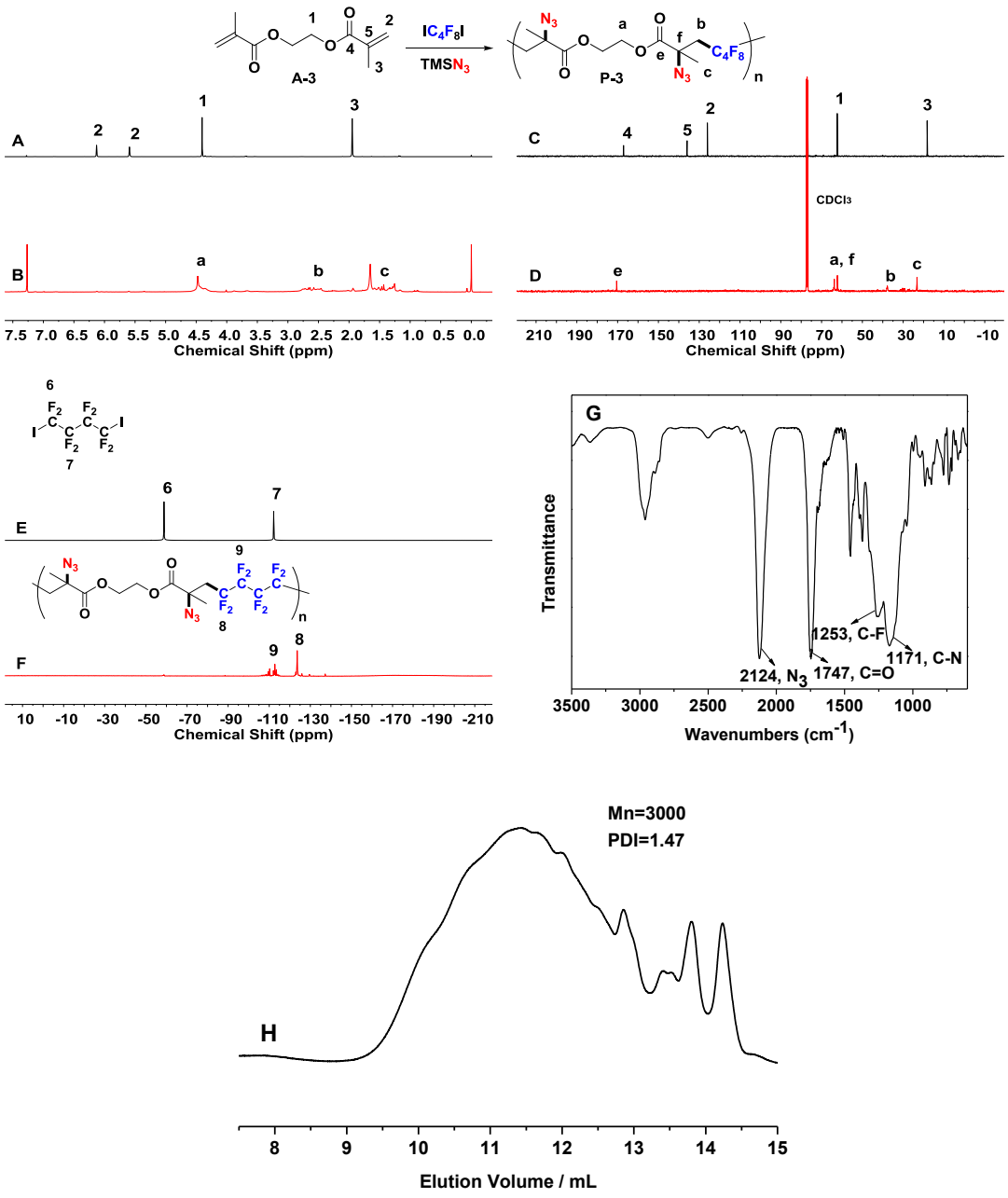

Figure S15: ^{1}H NMR spectra (A: **A-3**; B: **P-3**); ^{13}C NMR spectra (C: **A-3**; D: **P-3**); ^{19}F NMR spectra (E: 1,4-diiodoperfluorobutane; F: **P-3**); FT-IR spectrum of **P-3** (G). GPC curve of **P-3** (H), related to **Table 1.**

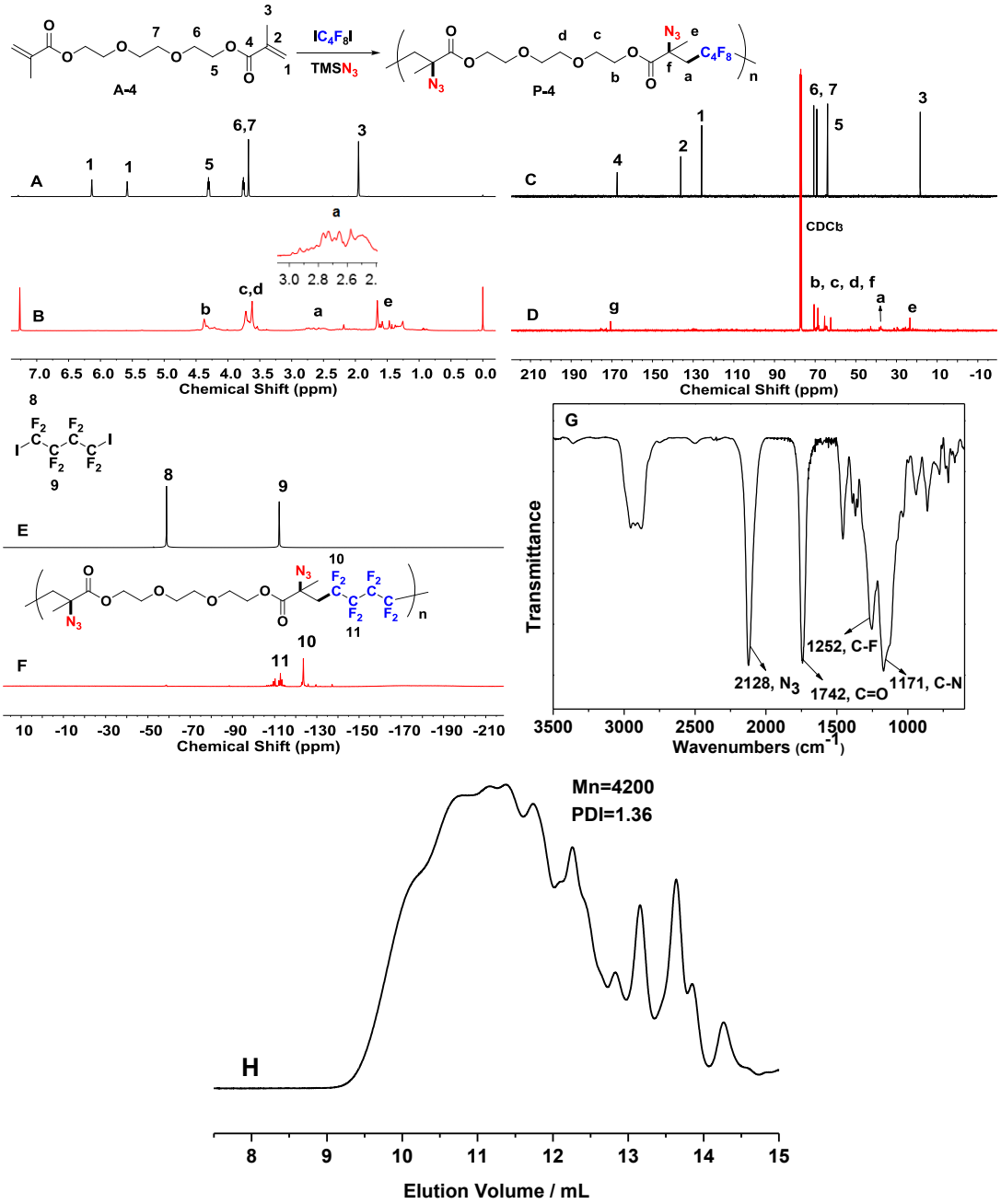

Figure S16: ^{1}H NMR spectra (A: **A-4**; B: **P-4**); ^{13}C NMR spectra (C: **A-4**; D: **P-4**); ^{19}F NMR spectra (E: 1,4-diiodoperfluorobutane; F: **P-4**); FT-IR spectrum of **P-4** (G). GPC curve of **P-4** (H), related to **Table 1.**

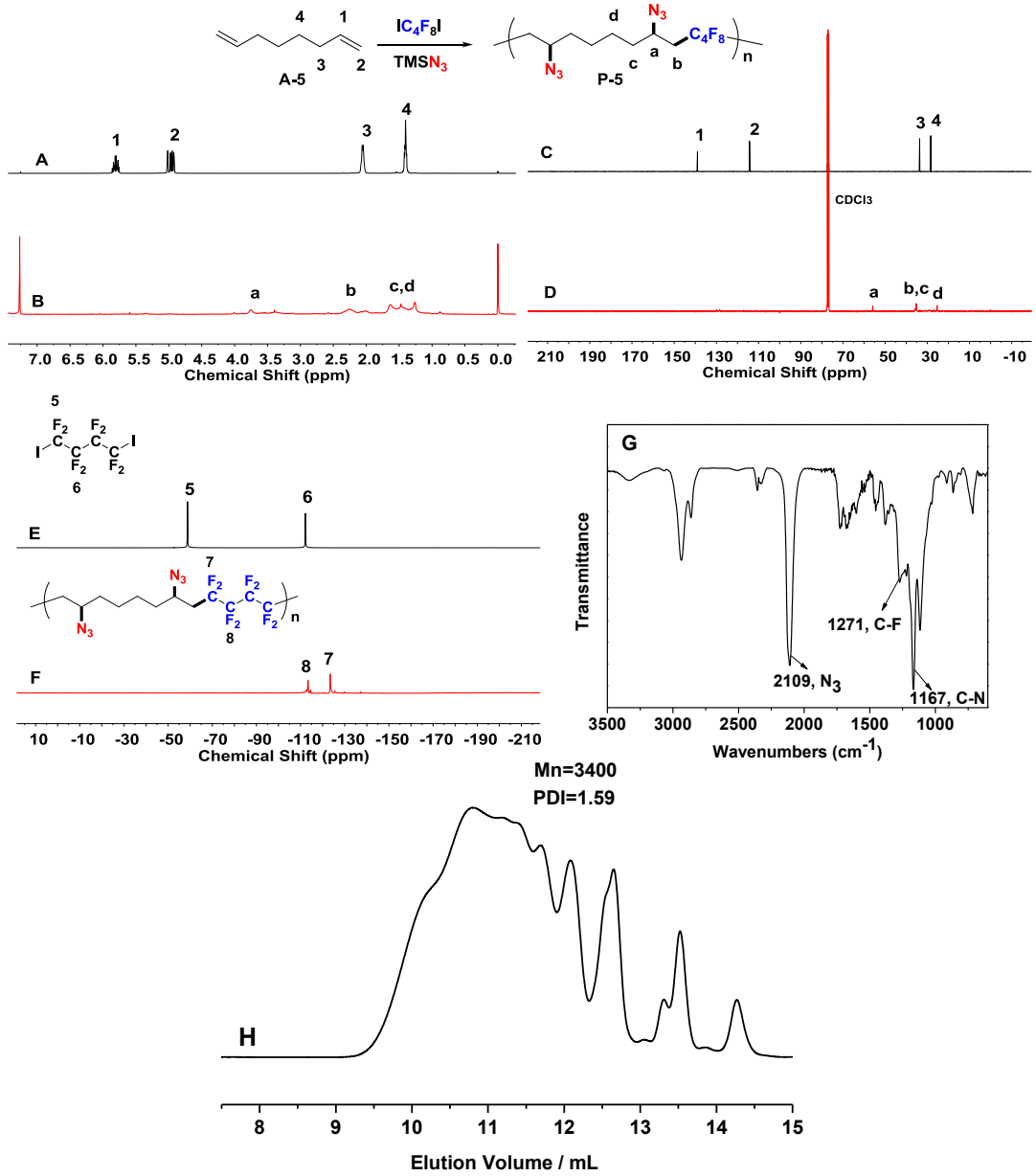

Figure S17: ^{1}H NMR spectra (A: **A-5**; B: **P-5**); ^{13}C NMR spectra (C: **A-5**; D: **P-5**); ^{19}F NMR spectra (E: 1,4-diiodoperfluorobutane; F: **P-5**); FT-IR spectrum of **P-5** (G), GPC curve of **P-5** (H), related to **Table 1.**

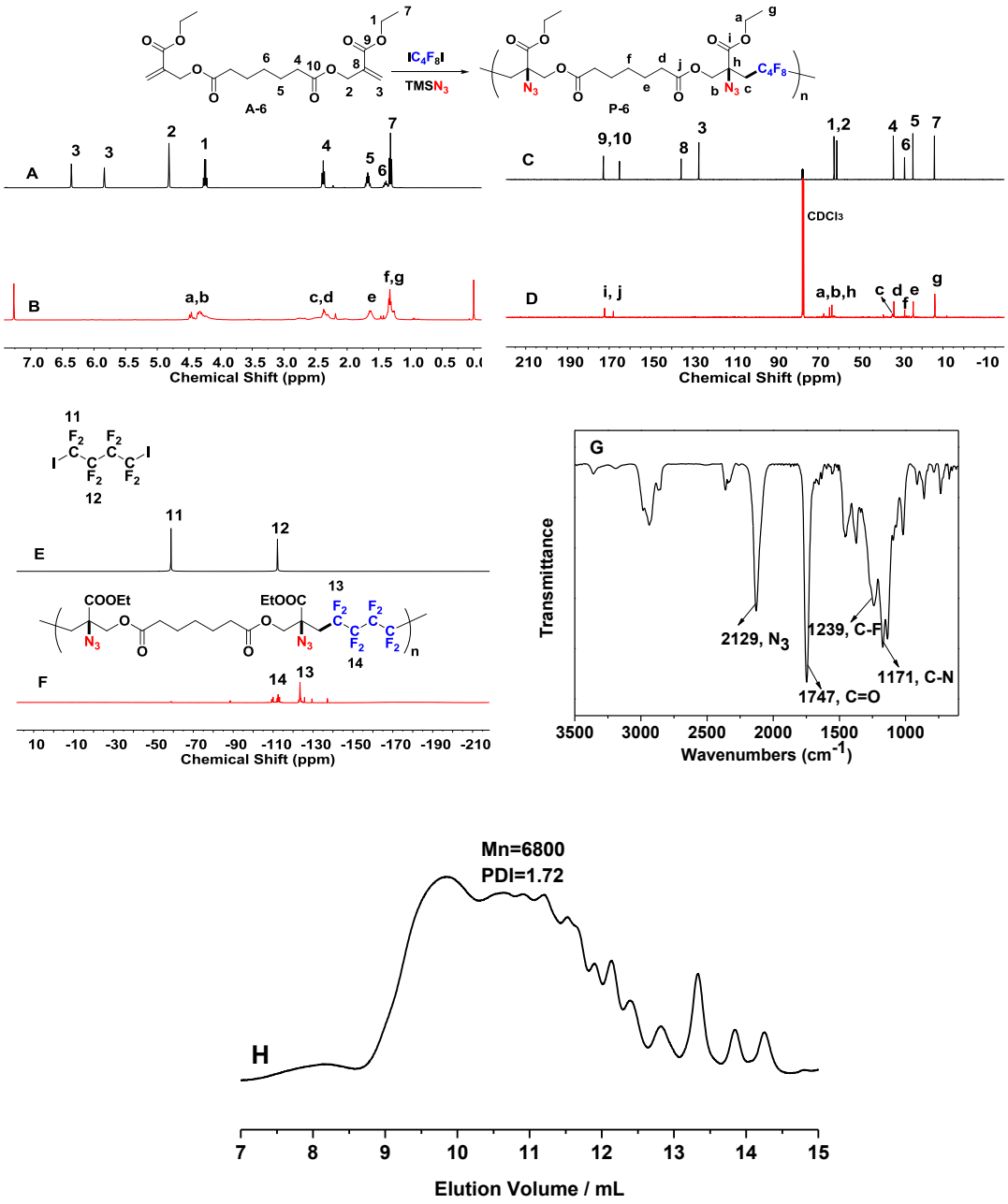

Figure S18: ^{1}H NMR spectra (A: **A-6**; B: **P-6**); ^{13}C NMR spectra (C: **A-6**; D: **P-6**); ^{19}F NMR spectra (E: 1,4-diiodoperfluorobutane; F: **P-6**); FT-IR spectrum of **P-6** (G), GPC curve of **P-6** (H). related to **Table 1.**

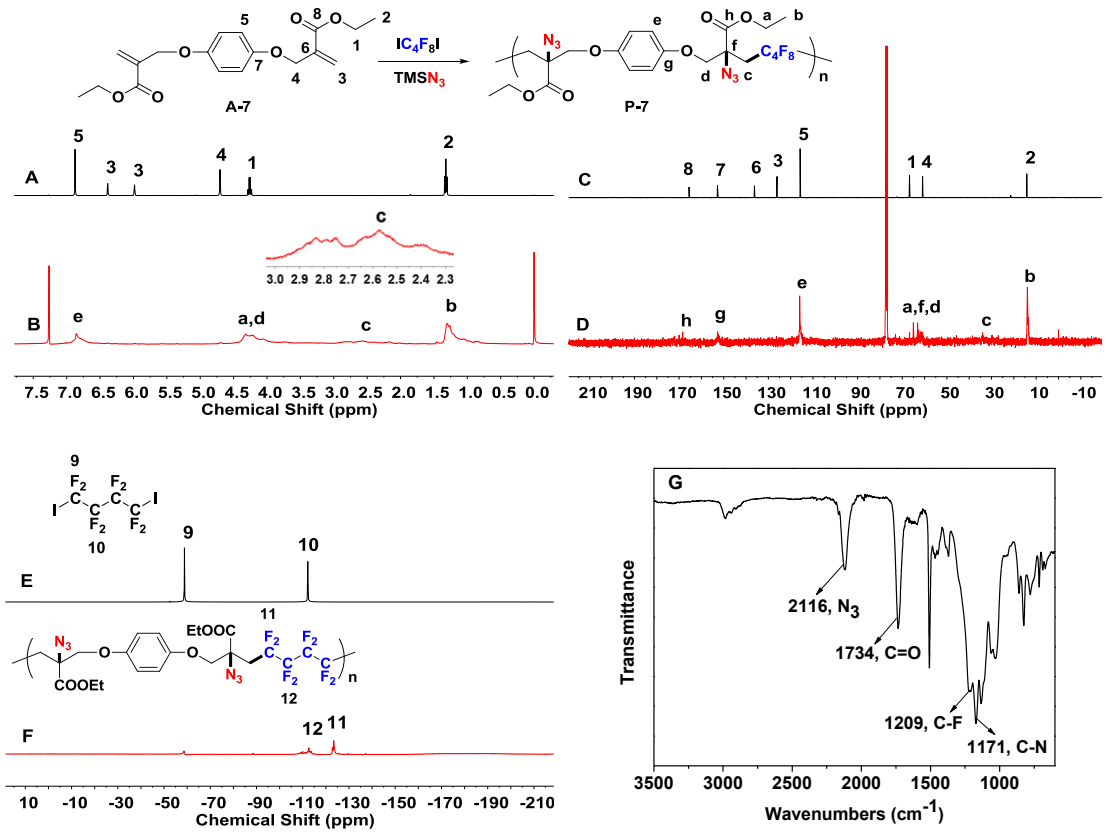

Figure S19: ^{1}H NMR spectra (A: **A-7**; B: **P-7**); ^{13}C NMR spectra (C: **A-7**; D: **P-7**); ^{19}F NMR spectra (E: 1,4-diiodoperfluorobutane; F: **P-7**); FT-IR spectrum of **P-7** (G), related to **Table 1.**

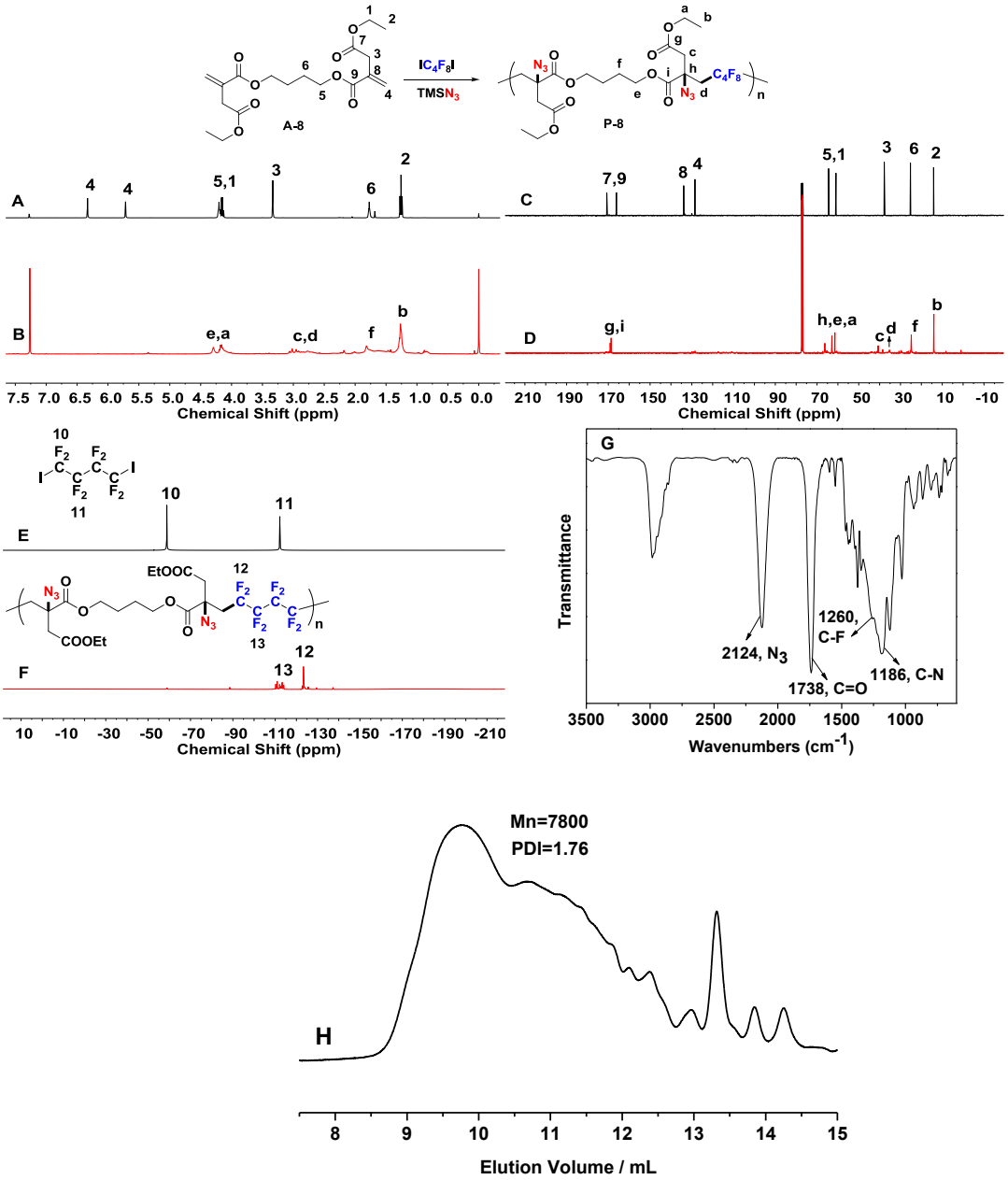

Figure S20: ^{1}H NMR spectra (A: **A-8**; B: **P-8**); ^{13}C NMR spectra (C: **A-8**; D: **P-8**); ^{19}F NMR spectra (E: 1,4-diiodoperfluorobutane; F: **P-8**); FT-IR spectrum of **P-8** (G). GPC curve of **P-8** (H), related to **Table 1.**

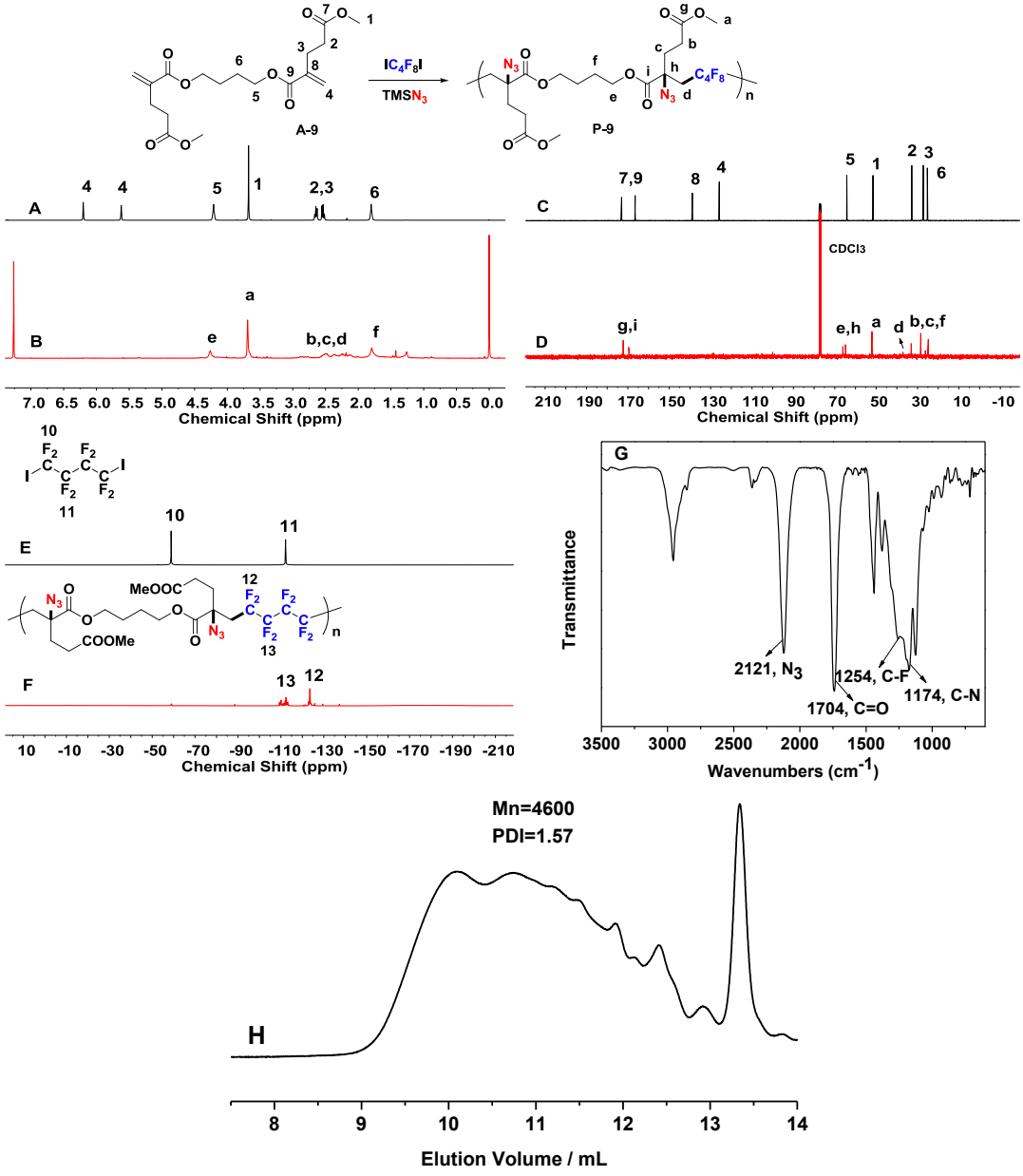

Figure S21: ^{1}H NMR spectra (A: **A-9**; B: **P-9**); ^{13}C NMR spectra (C: **A-9**; D: **P-9**); ^{19}F NMR spectra (E: 1,4-diiodoperfluorobutane; F: **P-9**); FT-IR spectrum of **P-9** (G). GPC curve of **P-9** (H), related to **Table 1.**

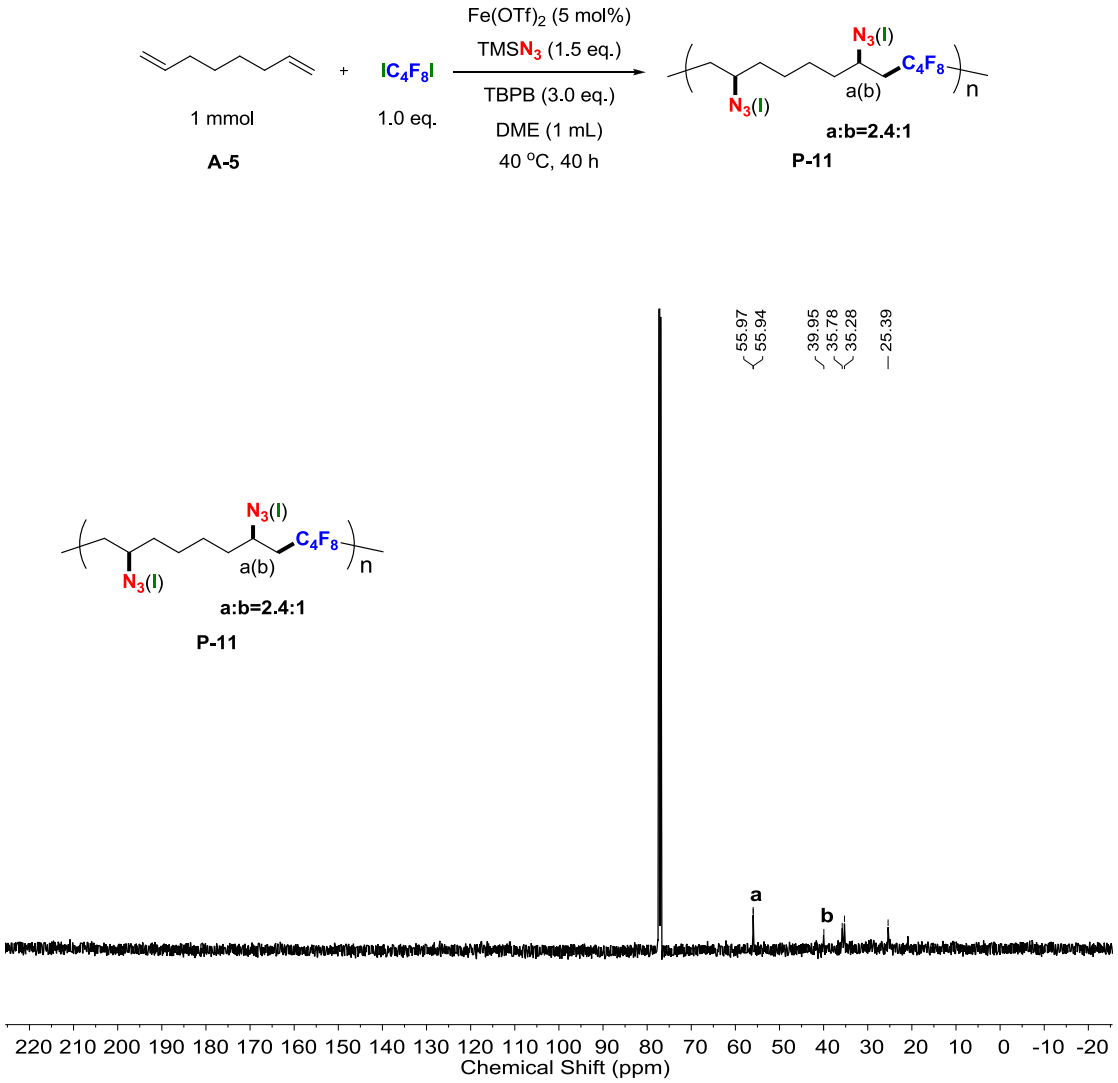

Figure S22: ^{13}C NMR spectrum of **P-11**, related to **Figure 2.**

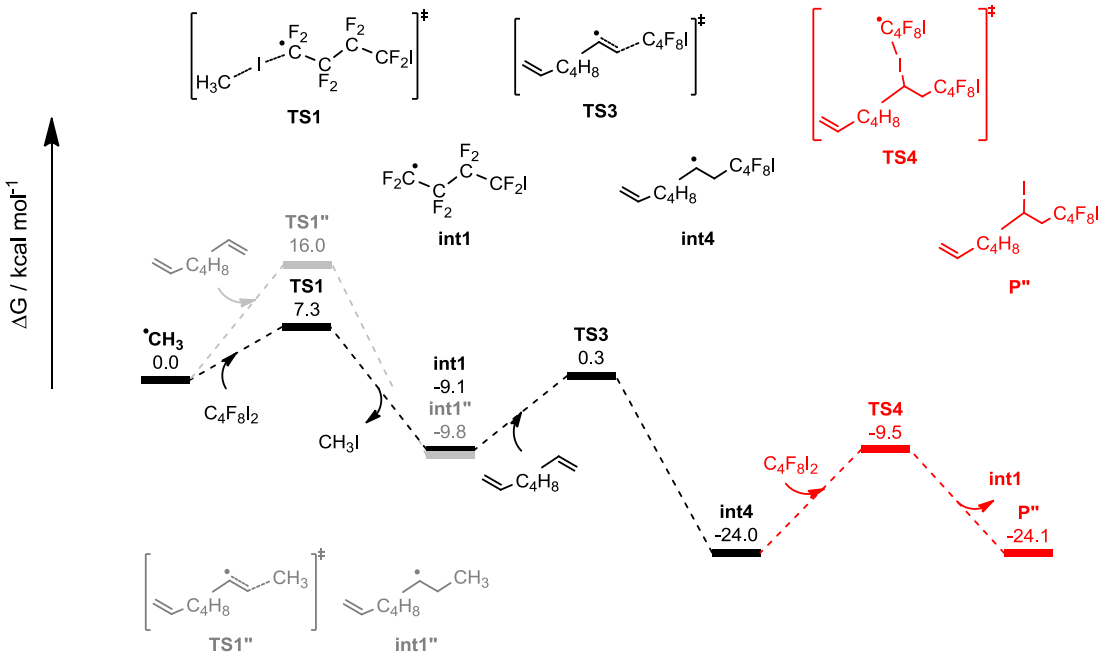

Figure S23: The free energy profile of radical cascade reactions (RCR) involving octa-1,7-diene, related to **Figure 4**.

Supplemental Tables

Table S1: chemicals and reagents, related to **Table 1.**

Alkenes	Company	Alkenes	Company
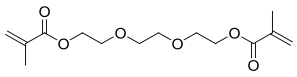	Energy	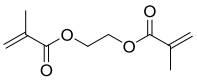	Energy
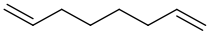	TCI	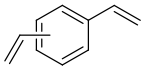	Energy
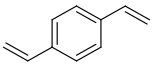	Ref[(Gauler and Risch, 1998)]		

Table S2: Electronic potential energies and correction to zero point energies, thermal energies, enthalpies, free energies (in Hartree) and imaginary frequencies (cm^{-1}) of optimized structures calculated at the B3LYP-D3/Def2-TZVP/(SMD-DME)//B3LYP-D3/Def2-SVP, related to **Figure 4.**

Entry	Structure	$E_{0,sol}$	$E_{0,gas}$	$cZPE_{298,gas}$	$cU_{298,gas}$	$cH_{298,gas}$	$cG_{298,gas}$	Imaginary Frequency
1	CH_3	-39.860112	-39.809533	0.029384	0.032479	0.033423	0.009546	
2	$C_4F_8I_2$	-1547.166601	-1545.992430	0.048245	0.062374	0.063318	0.003196	
3	**TS1**	-1587.029020	-1585.806085	0.080794	0.098316	0.099260	0.026628	-194.1464
4	**int1**	-1249.304365	-1248.142518	0.046553	0.059175	0.060119	0.003641	
5	CH_3I	-337.738235	-337.675604	0.036197	0.039386	0.040331	0.010417	
6	1,4-divinylbenzene	-387.213853	-386.786608	0.166125	0.175249	0.176194	0.131222	
7	**TS1'**	-427.071701	-426.596410	0.198351	0.210336	0.211280	0.158575	-277.7003
8	**int1'**	-427.130784	-426.661644	0.204433	0.215252	0.216196	0.166881	
9	**int2**	-1636.580988	-1635.001002	0.216344	0.238356	0.239300	0.160461	
10	$\mathbf{Fe^{III}N_3}$	-4490.549692	-4487.360850	0.435082	0.480612	0.481556	0.350644	
11	**int3**	-6127.143891	-6122.393287	0.653113	0.722376	0.723320	0.537355	
12	^{7}**MECP**	-6127.143600	-6122.392388					
13	^{5}**MECP**	-6127.143659	-6122.392555					
14	**P**	-1800.876122	-1799.105518	0.233181	0.258064	0.259008	0.172626	
15	**TS2**	-3183.735859	-3180.983660	0.265616	0.303733	0.304677	0.179546	-94.0418
16	**P'**	-1934.429575	-1932.837980	0.219390	0.243225	0.244169	0.159437	
17	octa-1,7-diene	-313.381642	-313.029914	0.198267	0.208225	0.209169	0.162294	
18	**TS1"**	-353.234366	-352.835316	0.230847	0.243511	0.244456	0.189876	-389.5851
19	**int1"**	-353.280079	-352.887510	0.235373	0.247541	0.248486	0.194576	
20	**TS3**	-1562.688345	-1561.179150	0.245236	0.269011	0.269955	0.183373	-164.5514
21	**int4**	-1562.732438	-1561.228537	0.247619	0.270836	0.271780	0.188702	
22	**TS4**	-3109.900185	-3107.229354	0.298190	0.336511	0.337455	0.216133	-150.6131
23	**P"**	-1860.597726	-1859.082790	0.252179	0.276606	0.277550	0.191216	

Transparent Methods

Materials and methods

All reactions were carried out under an atmosphere of nitrogen in flame-dried glassware with magnetic stirring unless otherwise indicated. Commercially obtained reagents were used as received. Solvents were dried by Innovative Technology Solvent Purification System. Liquids and solutions were transferred via syringe. ^{1}H, ^{13}C and ^{19}F NMR spectra were recorded on Bruker-BioSpin AVANCE III HD or ECZ600S. Data for ^{1}H NMR spectra are reported relative to chloroform (7.26 ppm) as an internal standard and are reported as follows: chemical shift (ppm), multiplicity, coupling constant (Hz), and integration. Data for ^{13}C NMR spectra are reported relative to chloroform (77.23 ppm) as an internal standard and are reported in terms of chemical shift (ppm). Fourier transform infrared (FT-IR) spectra were measured on a Bruker Vertex 70 FT-IR spectrometer (KBr disk). Gel permeation chromatography (GPC) for polymer molecular weight analysis was carried out with TOSOH HLC-8320 system equipped with an refractive index (RI) detector, using polystyrenes as standards and THF was used as the eluent in a flow rate of 1.0 mL/min.

Raw Materials

The chemicals and reagents were purchased from following companies (**Table S1**) or synthesized following corresponding supplemental references:

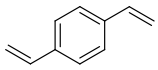

^{1}H NMR (400 MHz, $CDCl_3$) δ (ppm) δ 7.36 (s, 4H), 6.69 (dd, *J* = 17.6, 10.9 Hz, 2H), 5.74 (d, *J* = 17.6 Hz, 2H), 5.23 (d, *J* = 10.9 Hz, 2H). ^{13}C NMR (101 MHz, $CDCl_3$) δ 137.12, 136.49, 126.42, 113.78.

Other materials were synthesized following corresponding procedure:

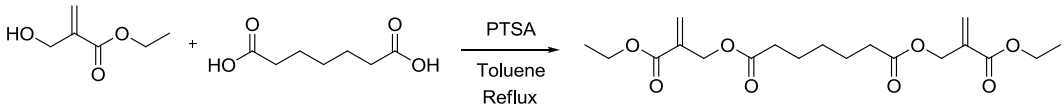

A mixture of ethyl 2-(hydroxymethyl)acrylate (2600 mg, 20 mmol, 2.5 eq.), pimelic acid (1280 mg, 4.0 mmol, 1.0 eq.), *p*-toluenesulfonic acid (0.2 mmol, 38 mg, 0.05 eq.) and toluene (50 mL) was refluxed with a Dean-Stark trap until the completion of water released. The organic layer concentrated by rotary evaporator under reduced pressure and the residue was purified by column chromatography on silica gel (PE:EA=10:1-3:1) to yield product as clean oil (2800 mg, 91% yield). ^{1}H NMR (400 MHz, $CDCl_3$) δ (ppm) 6.36 (s, 2H), 5.84 (d, *J* = 0.9 Hz, 2H), 4.82 (s, 4H), 4.24 (q, *J* = 7.1 Hz, 4H), 2.38 (t, *J* = 7.5 Hz,

4H), 1.78 – 1.59 (m, 4H), 1.44 – 1.36 (m, 2H), 1.32 (t, *J* = 7.1 Hz, 6H). ^{13}C NMR (101 MHz, $CDCl_3$) δ (ppm) 172.73, 165.03, 135.49, 126.99, 62.21, 60.86, 33.79, 28.40, 24.41, 14.07.

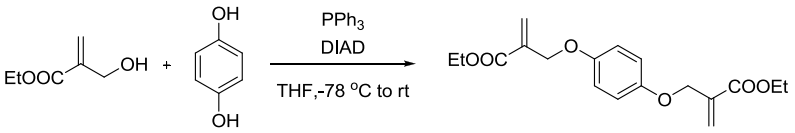

Ethyl 2-(hydroxymethyl)acrylate (2.73 g, 21 mmol, 2.1 eq.), 1,4-dihydroxybenzene (1.1 g, 10 mmol, 1.0 eq.) and triphenylphosphine (6.25 g, 24 mmol, 2.4 eq.) and THF (100 mL) were added to the single necked flask with a stirring bar under nitrogen protection. The solution was stirred at 0 °C and diisopropylazodicarboxylate (DIAD, 4.65 g, 24 mmol, 2.4 eq.) was added dropwise to the mixture. The solution was stirred at room temperature overnight. Then, the solution was concentrated by rotary evaporator under reduced and the residue was purified by column chromatography on silica gel (PE:EA=8:1-2:1) to yield product as white solid (601 mg, 36% yield). ^{1}H NMR (400 MHz, $CDCl_3$) δ (ppm) 6.87 (s, 4H), 6.39 (d, *J* = 1.1 Hz, 2H), 5.98 (d, *J* = 1.4 Hz, 2H), 4.70 (s, 4H), 4.26 (q, *J* = 7.1 Hz, 4H), 1.32 (t, *J* = 7.1 Hz, 6H). ^{13}C NMR (101 MHz, $CDCl_3$) δ (ppm) 165.54, 152.82, 136.23, 126.13, 115.77, 66.76, 60.91, 14.21.

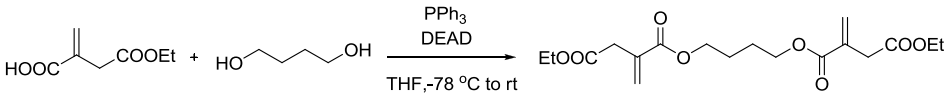

Monoethyl itaconate (1595 mg, 10.1 mmol, 2.02 eq.), 1,4-Butanediol (450 mg, 5 mmol, 1.0 eq.), triphenylphosphine (2882 mg, 11 mmol, 2.2 eq.) and THF (40 mL) were added to the single necked flask with a stirring bar under nitrogen protection. The solution was stirred at -78 °C and diethyl azodicarboxylate (DEAD, 1914 mg, 11 mmol, 2.2 eq.) was added dropwise to the mixture. The solution was stirred at -78 °C for 30 min and room temperature for 1 hour. Then, the solution was concentrated by rotary evaporator under reduced and the residue was purified by column chromatography on silica gel (PE:EA=8:1-2:1) to yield product as white solid (1221 mg, 66% yield). ^{1}H NMR (400 MHz, $CDCl_3$) δ (ppm) 6.33 (s, 2H), 5.72 (s, 2H), 4.28 – 4.09 (m, 8H), 3.33 (s, 4H), 1.77 (t, *J* = 2.8 Hz, 4H), 1.26 (t, *J* = 7.1 Hz, 6H). ^{13}C NMR (101 MHz, $CDCl_3$) δ (ppm) δ 170.73, 166.12, 133.87, 128.48, 64.46, 60.92, 37.77, 25.23, 14.14.

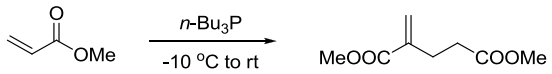

The synthesis method was following the supplemental reference.[(Tello-Aburto et al., 2014)] Methyl acrylate (4.5 mL, 50 mmol, 1.0 eq.) were added to the single necked flask with a stirring bar under nitrogen protection and cooed to -10 °C. Tributylphosphine (n-Bu_3P, 1.24 mL, 5.0 mmol, 0.1 eq.) was added to the flask slowly and stirred for 30 min. Then, the reaction mixture was then stirred at room temperature

for 4 hours before excess acrylate was removed in rotary evaporator under reduced. The residue was purified by column chromatography on silica gel (PE:EA=40:1-5:1) to yield product as clean oil (2.4 g, 56% yield). ^{1}H NMR (400 MHz, $CDCl_3$) δ (ppm) 6.20 (s, 1H), 5.61 (d, *J* = 1.0 Hz, 1H), 3.77 (s, 3H), 3.68 (s, 3H), 2.65 (t, *J* = 7.4 Hz, 1H), 2.53 (t, *J* = 7.2 Hz, 1H). ^{13}C NMR (101 MHz, $CDCl_3$) δ (ppm) δ 172.99, 166.97, 138.71, 125.86, 51.79, 51.48, 32.78, 27.24.

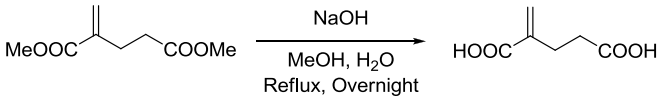

The synthesis method was following the supplemental reference.[(Tello-Aburto et al., 2014)] Dimethyl ester (1 g, 5.8 mmol), methanol (6 mL), water (3 mL) and NaOH (697 mg, 17.4 mmol) were added to the single necked flask with a stirring bar. The flask was adapted to a condenser, and the solution refluxed overnight. The solution was then cooled to room temperature and acidified with 6N HCl solution. The solution was extracted with ethyl acetate. The organic layer was dried over $MgSO_4$, filtered and concentrated to give 818 mg of a white solid in 98% yield.

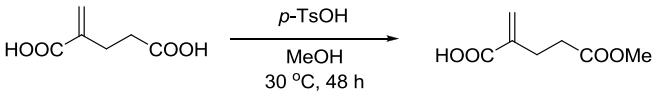

The synthesis method was following the supplemental reference.[(Tello-Aburto et al., 2014)] 2-methylenepentanedioic acid (1 g, 6.9 mmol), methanol (20 mL), and *p*-Toluenesulfonamide (*p*-TsOH, 60 mg, 0.34 mmol) were added to the single necked flask with a stirring bar. The solution was stirred at room temperature for 48 hours before concentrating in rotary evaporator under reduced. The residue was purified by column chromatography on silica gel (PE:EA=5:1-1:1) to yield product as clean oil (905 mg, 83% yield).

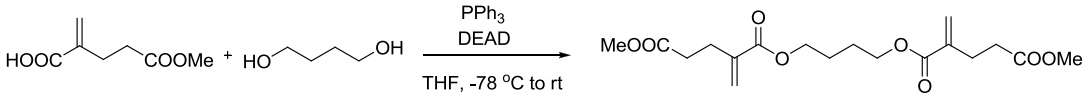

5-methoxy-2-methylene-5-oxopentanoic acid (1595 mg, 10.1 mmol, 2.02 eq.), 1,4-Butanediol (450 mg, 5 mmol, 1.0 eq.) and triphenylphosphine (2882 mg, 11 mmol, 2.2 eq.) and THF (20 mL) were added to the single necked flask with a stirring bar under nitrogen protection. The solution was stirred at -78 °C and diethyl azodicarboxylate (DEAD, 1914 mg, 11 mmol, 2.2 eq.) was added dropwise to the mixture. The solution was stirred at -78 °C for 1 hour and room temperature for 3 hours. Then, the solution was concentrated by rotary evaporator under reduced and the residue was purified by column chromatography on silica gel (PE:EA=10:1-5:1) to yield product as clean oil (1202 mg, 65% yield). ^{1}H NMR (400 MHz, $CDCl_3$) δ (ppm) 6.20 (s, 2H), 5.62 (d, *J* = 0.9 Hz, 2H), 4.21 (t, *J* = 4.9 Hz, 4H), 3.68 (s, 6H), 2.65 (t, *J* = 7.4 Hz, 4H), 2.54 (t, *J* = 7.1 Hz, 4H), 1.86-1.75 (m, 4H). ^{13}C NMR (101 MHz,

$CDCl_3$) δ (ppm) 173.02, 166.47, 138.83, 125.83, 64.20, 51.55, 32.80, 27.21, 25.29.

Polymerization

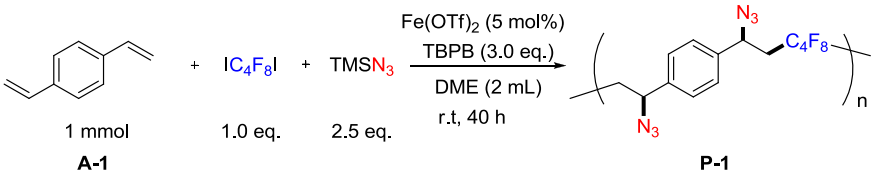

$Fe(OTf)_2$ (17.7 mg, 5 mol%) and 0.5 mL DME were added into a flame dried schlenk tube with a stirring bar under nitrogen protection. The mixture of alkene (**A-1**) (130 mg, 1 mmol, 1.0 equiv), IC_4F_8I (453 mg, 1.0 eq.), $TMSN_3$ (287.5 mg, 2.5 eq.), TBPB (582 mg, 3.0 eq.) and DME (0.5 mL) was added to the schlenk tube drop by drop at r.t. The reaction mixture was stirred for 40 hours and then workup with dichloromethane/water. The organic solution was dried with anhydrous $MgSO_4$ and concentrated under reduced pressure. The mixture was diluted with 1.5 mL THF, and then precipitated in 60 mL of petroleum ether. The precipitates were filtered and washed with petroleum ether and dried under vacuum to a constant weight. 157 mg polymer (**P-1**) was obtained as a viscous brown solid with a yield of 38%. *M*n: 5100, *M*w: 9100, *Đ*: 1.78. ^{1}H NMR (400 MHz, $CDCl_3$) δ (ppm): 7.47-7.32 (broad, 4H), 5.06-4.72 (broad, 2H), 2.63-2.36 (broad, 4H). ^{13}C NMR (101 MHz, $CDCl_3$) δ (ppm): 139.22, 127.52, 126.92, 58.62, 37.59 (m). ^{19}F NMR (376 MHz, $CDCl_3$) δ (ppm): -113.27 (s, 2F), -123.34 (s, 2F). FT-IR (KBr disk), *v* (cm^{-1}): 2927, 2855, 2109, 1427, 1378, 1246, 1168, 1106, 844, 734.

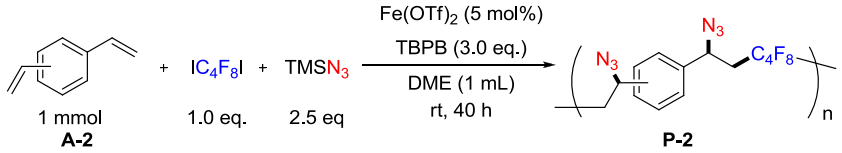

$Fe(OTf)_2$ (17.7 mg, 5 mol%) and 0.5 mL DME were added into a flame dried schlenk tube with a stirring bar under nitrogen protection. The mixture of alkene (**A-2)** (130 mg, 1 mmol, 1.0 equiv), IC_4F_8I (453 mg, 1.0 eq.), $TMSN_3$ (287.5 mg, 2.5 eq.), TBPB (582 mg, 3.0 eq.) and DME (0.5 mL) was added to the schlenk tube drop by drop at r.t. The reaction mixture was stirred for 40 hours and then workup with dichloromethane/water. The organic solution was dried with anhydrous $MgSO_4$ and concentrated under reduced pressure. The mixture was diluted with 1.5 mL THF, and then precipitated in 60 mL of petroleum ether. The precipitates were filtered and washed with petroleum ether and dried under vacuum to a constant weight. 203 mg polymer (**P-2**) was obtained as a viscous brown solid with a yield of 48%. *M*n: 4300, *M*w: 6600, *Đ*: 1.53. ^{1}H NMR (400 MHz, $CDCl_3$) δ (ppm): 7.48-7.28 (broad, 4H), 5.09-4.72 (broad, 2H), 2.64-2.39 (broad, 4H). ^{13}C NMR (101 MHz, $CDCl_3$) δ (ppm): 139.52, 139.21,

130.20, 127.51, 127.25, 124.89, 58.81, 37.65 (m). ^{19}F NMR (376 MHz, $CDCl_3$) δ (ppm): -113.17 (s, 2F), -123.35 (s, 2F). FT-IR (KBr disk), *v* (cm^{-1}): 2927, 2108, 1417, 1246, 1168, 1117, 708.

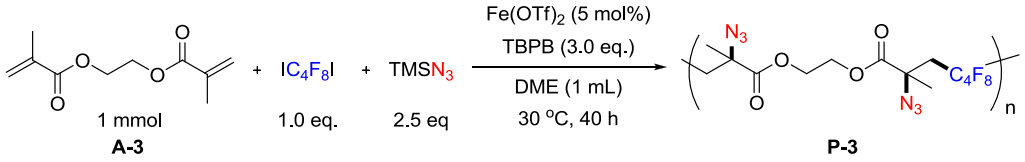

$Fe(OTf)_2$ (17.7 mg, 5 mol%) and 0.5 mL DME were added into a flame dried schlenk tube with a stirring bar under nitrogen protection. The mixture of alkene (**A-3)** (198 mg, 1 mmol, 1.0 equiv), IC_4F_8I (453 mg, 1.0 eq.), $TMSN_3$ (287.5 mg, 2.5 eq.), TBPB (582 mg, 3.0 eq.) and DME (0.5 mL) was added to the schlenk tube drop by drop at r.t. The reaction mixture was stirred for 40 hours and then workup with dichloromethane/water. The organic solution was dried with anhydrous MgSO4 and concentrated under reduced pressure. The mixture was diluted with 1.5 mL THF, and then precipitated in 60 mL of petroleum ether. The precipitates were filtered and washed with petroleum ether and dried under vacuum to a constant weight. 242 mg polymer (**P-3)** was obtained as a viscous brown solid with a yield of 50%. *M*n: 3000, *M*w: 4400, *Đ*: 1.47. ^{1}H NMR (400 MHz, $CDCl_3$) δ (ppm): 4.57-4.29 (broad, 4H), 2.89-2.41 (broad, 4H), 1.65-1.08 (broad, 6H). ^{13}C NMR (101 MHz, $CDCl_3$) δ (ppm): 170.50, 63.75, 62.25, 37.98 (m), 23.23. ^{19}F NMR (376 MHz, $CDCl_3$) δ (ppm): -112.73 (m, 2F), -123.69 (m, 2F). FT-IR (KBr disk), *v* (cm^{-1}): 2961, 2124, 1747, 1456, 1369, 1253, 1171.

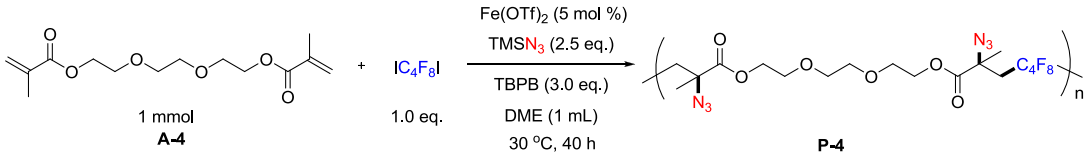

$Fe(OTf)_2$ (17.7 mg, 5 mol%) and 0.5 mL DME were added into a flame dried schlenk tube with a stirring bar under nitrogen protection. The mixture of alkene (**A-4)** (286 mg, 1 mmol, 1.0 equiv), IC_4F_8I (453 mg, 1.0 eq.), $TMSN_3$ (287.5 mg, 2.5 eq.), TBPB (582 mg, 3.0 eq.) and DME (0.5 mL) was added to the schlenk tube drop by drop at r.t. The reaction mixture was stirred for 40 hours and then workup with dichloromethane/water. The organic solution was dried with anhydrous MgSO4 and concentrated under reduced pressure. The mixture was diluted with 1.5 mL THF, and then precipitated in 60 mL of petroleum ether. The precipitates were filtered and washed with petroleum ether and dried under vacuum to a constant weight. 340 mg polymer (**P-4)** was obtained as a viscous brown solid with a yield of 60%. *M*n: 4200, *M*w: 5700, *Đ*: 1.36. ^{1}H NMR (400 MHz, $CDCl_3$) δ (ppm): 4.42-4.14(broad, 4H), 3.74-3.55 (broad, 8H), 2.98-2.34 (broad, 4H), 1.62-1.24 (broad, 6H). ^{13}C NMR (101 MHz, $CDCl_3$) δ (ppm): 170.64, 70.52, 68.67, 65.33, 62.33, 37.72, 23.38. ^{19}F NMR (376 MHz, $CDCl_3$) δ (ppm): -112.75 (m, 2F), -123.61 (m, 2F). FT-IR (KBr disk), *v* (cm^{-1}): 2878, 2173, 1457, 1253, 1171, 941, 862.

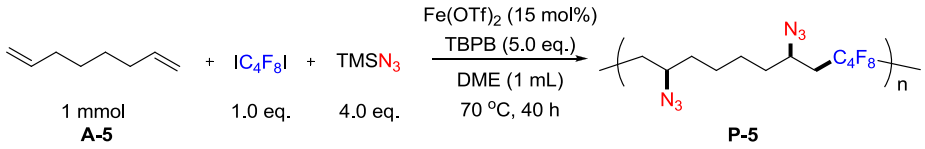

$Fe(OTf)_2$ (53.1 mg, 15 mol%) and 0.5 mL DME were added into a flame dried schlenk tube with a stirring bar under nitrogen protection. The mixture of alkene (**A-5)** (110 mg, 1 mmol, 1.0 equiv), IC_4F_8I (453 mg, 1.0 eq.), $TMSN_3$ (460 mg, 4.0 eq.), TBPB (970 mg, 5.0 eq.) and DME (0.5 mL) was added to the schlenk tube drop by drop at 70 °C. The reaction mixture was stirred for 40 hours. Then, the reaction mixture was cooled to ambient temperature and workup with dichloromethane/water. The organic solution was dried with anhydrous $MgSO_4$ and concentrated under reduced pressure. The mixture was diluted with 1.5 mL THF, and then precipitated in 60 mL of petroleum ether. The precipitates were filtered and washed with petroleum ether and dried under vacuum to a constant weight. 230 mg polymer (**P-5)** was obtained as a viscous brown solid with a yield of 58%. *M*n: 3400, *M*w: 5400, *Đ*: 1.59. ^{1}H NMR (400 MHz, $CDCl_3$) δ (ppm): 3.85-3.48(broad, 2H), 2.36-1.98 (broad, 4H), 1.67-1.35 (broad, 8H). ^{13}C NMR (101 MHz, $CDCl_3$) δ (ppm): 55.89, 35.71, 35.22, 25.36. ^{19}F NMR (376 MHz, $CDCl_3$) δ (ppm): -113.42 (m, 2F), -123.42 (m, 2F). FT-IR (KBr disk), *v* (cm^{-1}): 2936, 2862, 2109, 1271, 1167, 1116, 715.

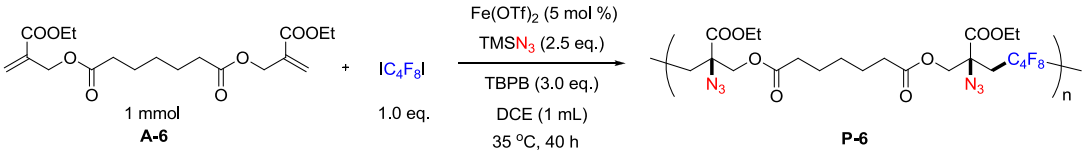

$Fe(OTf)_2$ (17.7 mg, 5 mol%) and 0.5 mL DME were added into a flame dried schlenk tube with a stirring bar under nitrogen protection. The mixture of alkene (**A-6)** (384 mg, 1 mmol, 1.0 equiv), IC_4F_8I (453 mg, 1.0 eq.), $TMSN_3$ (287.5 mg, 2.5 eq.), TBPB (582 mg, 3.0 eq.) and DME (0.5 mL) was added to the schlenk tube drop by drop at r.t. The reaction mixture was stirred for 40 hours and then workup with dichloromethane/water. The organic solution was dried with anhydrous $MgSO_4$ and concentrated under reduced pressure. The mixture was diluted with 1.5 mL THF, and then precipitated in 60 mL of petroleum ether. The precipitates were filtered and washed with petroleum ether and dried under vacuum to a constant weight. 434 mg polymer (**P-6)** was obtained as a viscous brown solid with a yield of 65%. *M*n: 6800, *M*w: 11700, *Đ*: 1.72. ^{1}H NMR (400 MHz, $CDCl_3$) δ (ppm): 4.54-4.06 (broad, 8H), 2.86-2.24 (broad, 8H), 1.74-1.57 (broad, 4H), 1.38-1.21 (broad, 8H). ^{13}C NMR (101 MHz, $CDCl_3$) δ (ppm): 172.19, 167.97, 67.09, 64.36, 63.21, 34.28, 34.08, 33.52, 28.29, 24.22, 13.89. ^{19}F NMR (376 MHz, $CDCl_3$) δ (ppm): -112.53 (s, 2F), -123.48 (s, 2F). FT-IR (KBr disk), *v* (cm^{-1}): 2937, 2129, 1747, 1456, 1372, 1239, 1171, 1136, 1018.

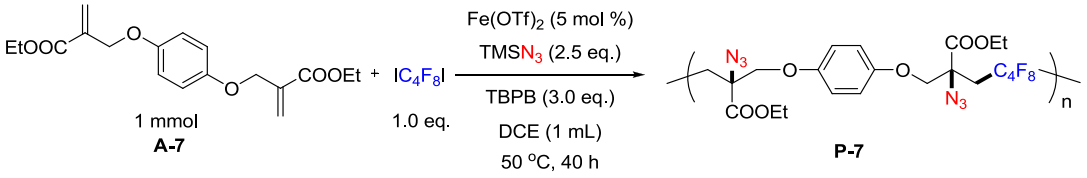

$Fe(OTf)_2$ (17.7 mg, 5 mol%) and 0.5 mL DME were added into a flame dried schlenk tube with a stirring bar under nitrogen protection. The mixture of alkene (**A-7)** (334 mg, 1 mmol, 1.0 equiv), IC_4F_8I (453 mg, 1.0 eq.), $TMSN_3$ (287.5 mg, 2.5 eq.), TBPB (582 mg, 3.0 eq.) and DME (0.5 mL) was added to the schlenk tube drop by drop at 50 °C. The reaction mixture was stirred for 40 hours. Then, the reaction mixture was cooled to ambient temperature and workup with dichloromethane/water. The organic solution was dried with anhydrous $MgSO_4$ and concentrated under reduced pressure. The mixture was diluted with 1.5 mL THF, and then precipitated in 60 mL of petroleum ether. The precipitates were filtered and washed with petroleum ether and dried under vacuum to a constant weight. 464 mg polymer (**P-7)** was obtained as a brown solid with a yield of 75%. ^{1}H NMR (400 MHz, $CDCl_3$) δ (ppm): 7.11-6.56 (broad, 4H), 4.57-3.76 (broad, 8H), 2.97-2.24 (broad, 4H), 1.37-1.11 (broad, 6H). ^{13}C NMR (101 MHz, $CDCl_3$) δ (ppm): 168.37, 152.73, 115.98, 66.74, 65.03, 63.13, 34.02, 13.94. ^{19}F NMR (376 MHz, $CDCl_3$) δ (ppm): -113.33 (m, 2F), -123.40 (m, 2F). FT-IR (KBr disk), *v* (cm^{-1}): 2983, 2116, 1734, 1507, 1209, 1171, 1134, 1032, 825, 713.

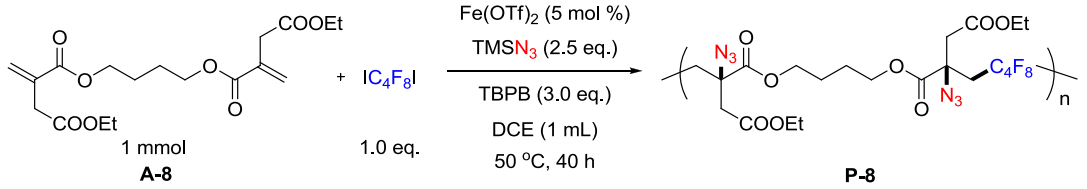

$Fe(OTf)_2$ (17.7 mg, 5 mol%) and 0.5 mL DME were added into a flame dried schlenk tube with a stirring bar under nitrogen protection. The mixture of alkene (**A-8)** (370 mg, 1 mmol, 1.0 equiv), IC_4F_8I (453 mg, 1.0 eq.), $TMSN_3$ (287.5 mg, 2.5 eq.), TBPB (582 mg, 3.0 eq.) and DME (0.5 mL) was added to the schlenk tube drop by drop at 50 °C. The reaction mixture was stirred for 40 hours. Then, the reaction mixture was cooled to ambient temperature and workup with dichloromethane/water. The organic solution was dried with anhydrous $MgSO_4$ and concentrated under reduced pressure. The mixture was diluted with 1.5 mL THF, and then precipitated in 60 mL of petroleum ether. The precipitates were filtered and washed with petroleum ether and dried under vacuum to a constant weight. 510 mg polymer (**P-8)** was obtained as a viscous brown solid with a yield of 78%. *M*n: 7800, *M*w: 13700, *Đ*: 1.76. ^{1}H NMR (400 MHz, $CDCl_3$) δ (ppm): 4.39-4.03 (broad, 8H), 3.09-2.54 (broad, 8H), 1.87-1.74 (broad, 4H), 1.29-1.25 (broad, 6H). ^{13}C NMR (101 MHz, $CDCl_3$) δ (ppm): 169.11, 168.68, 66.24, 62.88, 61.43, 40.71, 35.35, 24.82, 13.99. ^{19}F NMR (376 MHz, $CDCl_3$) δ (ppm): -112.71 (m, 2F), -123.35 (m, 2F). FT-IR (KBr disk), *v* (cm^{-1}): 2982, 2124, 1738, 1446, 1374, 1260, 1186, 1121, 1027, 935.

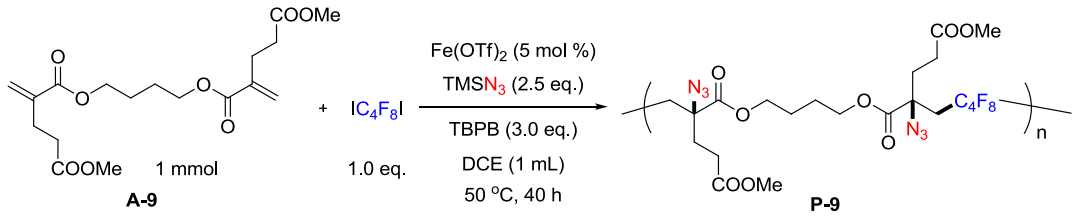

$Fe(OTf)_2$ (17.7 mg, 5 mol%) and 0.5 mL DME were added into a flame dried schlenk tube with a stirring bar under nitrogen protection. The mixture of alkene (**A-9)** (370 mg, 1 mmol, 1.0 equiv), IC_4F_8I (453 mg, 1.0 eq.), $TMSN_3$ (287.5 mg, 2.5 eq.), TBPB (582 mg, 3.0 eq.) and DME (0.5 mL) was added to the schlenk tube drop by drop at 50 °C. The reaction mixture was stirred for 40 hours. Then, the reaction mixture was cooled to ambient temperature and workup with dichloromethane/water. The organic solution was dried with anhydrous $MgSO_4$ and concentrated under reduced pressure. The mixture was diluted with 1.5 mL THF, and then precipitated in 60 mL of petroleum ether. The precipitates were filtered and washed with petroleum ether and dried under vacuum to a constant weight. 476 mg polymer (**P-9)** was obtained as a viscous brown solid with a yield of 73%. *M*n: 4600, *M*w: 7200, *Đ*: 1.57. ^{1}H NMR (400 MHz, $CDCl_3$) δ (ppm): 4.35-4.09 (broad, 4H), 3.73-3.63 (broad, 6H), 2.93-2.16 (broad, 12H), 1.83-1.73 (broad, 4H). ^{13}C NMR (101 MHz, $CDCl_3$) δ (ppm): 172.25, 169.53, 66.09, 64.82, 52.01, 37.00, 33.06, 28.46, 24.81. ^{19}F NMR (376 MHz, $CDCl_3$) δ (ppm): -112.36 (m, 2F), -123.51 (m, 2F). FT-IR (KBr disk), *v* (cm^{-1}): 2957, 2121, 1740, 1439, 1378, 1254, 1174, 1125.

Reduction and deprotection of poly(anmino acids) precursor

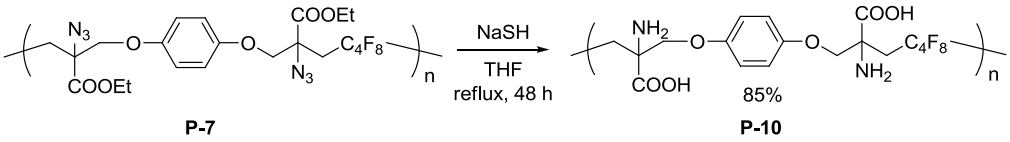

Polymer **P-7** (0.5 mmol, 309 mg, 1.0 equiv), NaSH (20 mmol, 1120 mg, 40 eq.) and THF (20 mL) were added into a round-bottomed flask with a stirring bar. The reaction mixture was heated to reflux for 48 hours. Then, the reaction mixture was cooled to ambient temperature and workup with dichloromethane/water. The pH of the water solution was adjusted to neutral. After stand still for 24 hours, a brown solid was precipitated. The precipitates were filtered and dried under vacuum to a constant weight. 434 mg polymer **P-10** was obtained as a viscous brown solid with a yield of 85%. FT-IR (KBr disk), *v* (cm^{-1}): 3385, 2960, 2921, 1626, 1507, 1259, 1097, 998, 797, 622.

Computational method and details

In this study, the hybrid density functional theory B3LYP[(Becke, 1993, Lee et al., 1988)] with Grimme's dispersion correction (DFT-D3)(Grimme et al., 2010, Grimme et al., 2011) was employed for all of geometrical optimizations, thermal energy calculations and frequency analyses. Basis sets Def2-SVP were employed here for all atoms.[(Weigend and Ahlrichs, 2005, Weigend, 2006)] Transition state structures were searched by simply performing a crude relaxed potential energy surface (RPES) scan connecting reactants and products, and then optimized by the rational function optimization (RFO) method of TS.[(Besalú and Bofill, 1998)] Furthermore, imaginary frequencies for all of transition states were verified to be the only one in theirs vibrations and were confirmed the correctness by viewing the normal mode vector. The intrinsic reaction coordinate (IRC) path calculations were also performed to confirm the connection from transition states to intermediates or products.[(Fukui, 1981)] All optimized stationary points were characterized by frequency calculation for identification of minimum points and saddle points. Then, single point solvated energies were calculated at the B3LYP-D3/Def2-TZVP[(Weigend and Ahlrichs, 2005, Weigend, 2006)] level of theory with SMD solvation model calculation in DME solution based upon the optimized structures,[(Marenich et al., 2009)] and the reported Gibbs free energy is obtained by adding the solution-phase electronic energy with the gas-phase Gibbs free energy correction for saving the computational time consumption. On the other hand, for benzyl and alkyl radical coupling with the sextet $Fe^{III}N_3$ species to grab the azide, the minimum energy crossing point (MECP) crossing the septet and quintet state was also located by using the hybrid approach method of Harvey.[(Harvey et al., 1998)] All calculations were performed by the Gaussian 09 package.[(Frisch et al., 2013)]

Coordinate of optimized structures

Structure S1. CH_3

E(B3LYP)sol = -39.8601119636 E(B3LYP)gas = -39.8095333169

6	0.000000	-0.000026	0.000255
1	-0.938485	-0.556488	-0.000510
1	0.951282	-0.534327	-0.000510
1	-0.012796	1.090973	-0.000510

Structure S2. $C_4F_8I_2$

E(B3LYP)sol = -1547.16660136 E(B3LYP)gas = -1545.99243017

6	0.716069	0.320103	0.009859
9	0.812442	1.203107	1.017921
9	0.876382	0.958595	-1.159511
6	1.850443	-0.737428	0.181183
9	1.794943	-1.250750	1.410548
9	1.679811	-1.719230	-0.707777
53	3.834461	0.180302	-0.116841
6	-0.716018	-0.319887	0.009569
6	-1.850445	0.737527	0.181429
53	-3.834450	-0.180447	-0.116822
9	-0.812527	-1.203543	1.017272
9	-0.876250	-0.957712	-1.160105
9	-1.679978	1.719585	-0.707636
9	-1.794918	1.250589	1.410610

Structure S3. TS1

E(B3LYP)sol = -1587.02901951 E(B3LYP)gas = -1585.80608450

6	-0.433094	-0.197180	0.060917
9	-0.564681	-0.962420	1.158835
9	-0.640821	-0.945697	-1.034739
6	-1.498433	0.926030	0.121127
9	-1.422110	1.582497	1.275846
9	-1.335403	1.778638	-0.889598
53	-3.658429	-0.005296	-0.028925
6	1.033311	0.353154	-0.011007
6	2.113427	-0.746353	0.225449
53	4.140491	0.047600	-0.148633
9	1.194406	1.305365	0.924398
9	1.207574	0.891049	-1.228601
9	1.887506	-1.776940	-0.593020
9	2.046664	-1.171963	1.486958
6	-5.963675	-1.145303	-0.311979
1	-6.221267	-1.315176	0.736679

1	-6.503691	-0.349726	-0.831987
1	-5.691783	-2.024069	-0.901868

Frequencies -- -194.1464

Red. masses -- 10.4902

Frc consts -- 0.2330

IR Inten -- 3.5630

Structure S4. int1

E(B3LYP)sol = -1249.30436511 E(B3LYP)gas = -1248.14251772

6	-2.026832	0.544073	0.119804
9	-2.114062	1.465041	-0.858973
9	-2.097865	1.148986	1.320718
6	-3.209915	-0.401118	-0.012704
9	-3.422651	-0.876466	-1.221336
9	-3.290903	-1.332009	0.915923
6	-0.643559	-0.180728	0.016016
6	0.579469	0.778857	-0.035845
53	2.475244	-0.354709	-0.009943
9	-0.653063	-0.926755	-1.105199
9	-0.533467	-0.988123	1.084681
9	0.543225	1.598685	1.017227
9	0.526239	1.505425	-1.152667

Structure S5. CH_3I

E(B3LYP)sol = -337.738234904 E(B3LYP)gas = -337.675603497

6	-1.841716	0.000003	-0.000066
1	-2.176791	-0.888710	-0.546994
1	-2.175209	-0.029724	1.043532
1	-2.176797	0.918400	-0.495537
53	0.331681	0.000000	-0.000011

Structure S6. 1,4-divinylbenzene

E(B3LYP)sol = -387.213853145 E(B3LYP)gas = -386.786607924

6	0.889447	-1.073353	0.000001
6	-0.483200	-1.299695	-0.000002
6	-1.409004	-0.236016	-0.000004
6	-0.889460	1.073306	-0.000004
6	0.483011	1.299552	-0.000001
6	1.409005	0.235760	0.000002
1	1.567346	-1.929564	0.000003
1	-0.855737	-2.328137	-0.000002
1	-1.567501	1.929378	-0.000006

1	0.855689	2.327959	0.000000
6	-2.849711	-0.535666	-0.000007
1	-3.092915	-1.604998	-0.000013
6	-3.867310	0.339515	-0.000003
1	-3.713648	1.422288	0.000004
1	-4.903891	-0.006174	-0.000005
6	2.849688	0.535625	0.000006
1	3.092451	1.605117	0.000005
6	3.867583	-0.339174	0.000009
1	3.713919	-1.421950	0.000010
1	4.903982	0.006955	0.000011

Structure S7. TS1'

E(B3LYP)sol = -427.071700529 E(B3LYP)gas = -426.596410056

6	1.494909	1.053155	0.267042
6	0.163915	1.441233	0.177414
6	-0.844965	0.545115	-0.244024
6	-0.445095	-0.771044	-0.561543
6	0.887389	-1.157987	-0.469434
6	1.893849	-0.260388	-0.055812
1	2.238246	1.782675	0.595739
1	-0.113815	2.466968	0.436696
1	-1.189191	-1.504606	-0.878936
1	1.164190	-2.185989	-0.720976
6	-2.230062	1.001537	-0.320099
1	-2.409805	2.013339	0.061131
6	-3.299642	0.288201	-0.760468
1	-3.187397	-0.678247	-1.255413
1	-4.285937	0.750899	-0.823271
6	-4.094550	-1.065499	1.198728
1	-3.131453	-1.543472	1.382835
1	-4.391269	-0.235727	1.841323
1	-4.872824	-1.631599	0.683366
6	3.286212	-0.725641	0.022533
1	3.431868	-1.776631	-0.254974
6	4.367499	-0.017803	0.387135
1	4.312223	1.035026	0.677805
1	5.358418	-0.477909	0.405846

Frequencies -- -277.7003

Red. masses -- 9.5754

Frc consts -- 0.4351

IR Inten -- 7.1976

Structure S8. int1'

E(B3LYP)sol = -427.130783744 E(B3LYP)gas = -426.661643721

6	1.474726	1.090887	0.109045
6	0.145798	1.449735	0.027839
6	-0.889076	0.482224	-0.198611
6	-0.465287	-0.878421	-0.334120
6	0.871872	-1.225447	-0.249531
6	1.885664	-0.262053	-0.026954
1	2.223110	1.867284	0.282494
1	-0.137840	2.500380	0.137594
1	-1.207833	-1.660371	-0.504312
1	1.158698	-2.275854	-0.356613
6	-2.236715	0.882560	-0.275729
1	-2.450136	1.946325	-0.123727
6	-3.406831	-0.034798	-0.464565
1	-3.153462	-0.841867	-1.174176
1	-4.237456	0.526461	-0.924937
6	-3.900173	-0.665545	0.853864
1	-3.103917	-1.265151	1.322652
1	-4.200007	0.110248	1.576369
1	-4.768057	-1.322131	0.678354
6	3.280439	-0.689615	0.052322
1	3.435903	-1.768574	-0.069142
6	4.367658	0.080388	0.252992
1	4.306005	1.164277	0.383407
1	5.366544	-0.360515	0.292718

Structure S9. int2

E(B3LYP)sol = -1636.58098801 E(B3LYP)gas = -1635.00100231

6	-6.369876	0.138328	-0.670105
6	-5.339925	1.047173	-0.787222
6	-4.106418	0.888776	-0.072292
6	-3.996190	-0.269403	0.760770
6	-5.037639	-1.173352	0.868632
6	-6.255586	-1.004043	0.165866
1	-7.289523	0.305003	-1.234861
1	-5.457815	1.917394	-1.438786
1	-3.068354	-0.461418	1.300835
1	-4.917725	-2.050404	1.511141
6	-3.088388	1.850020	-0.207932
1	-3.251074	2.670970	-0.911122
6	-1.773821	1.821139	0.507830
1	-1.854897	1.382892	1.512845
1	-1.373764	2.839808	0.624116
6	-7.319364	-1.993258	0.323057
1	-7.077369	-2.823683	0.997095
6	-8.534589	-1.990812	-0.258122
1	-8.859262	-1.202357	-0.942559

1	-9.250602	-2.792248	-0.061396
6	-0.709461	1.023965	-0.247912
6	0.675766	1.081384	0.456312
9	-0.560821	1.512762	-1.502350
9	-1.071118	-0.281921	-0.349753
9	1.130500	2.350522	0.367612
9	0.504349	0.782687	1.763299
6	1.746039	0.097143	-0.119562
6	3.195202	0.434541	0.348212
9	1.721342	0.140689	-1.461674
9	1.427463	-1.140216	0.294093
53	4.609907	-1.153046	-0.245852
9	3.213295	0.564972	1.678325
9	3.586191	1.583382	-0.204256

Structure S10. $Fe^{III}N_3$

E(B3LYP)sol = -4490.54969239 E(B3LYP)gas = -4487.36084973

26	-0.584317	-0.974223	0.312620
8	-2.817943	1.550377	1.251964
16	-3.108980	0.958953	-0.051873
8	-3.019012	1.800449	-1.252969
8	-2.422125	-0.407121	-0.255153
6	-4.881270	0.364037	0.005119
9	-5.694623	1.403852	0.159318
9	-5.185824	-0.263540	-1.131526
9	-5.046833	-0.477474	1.021918
8	2.405107	-3.571557	-0.603987
16	2.593557	-2.167558	-0.220195
8	1.319733	-1.548351	0.340222
8	3.763893	-1.798839	0.576402
6	2.833114	-1.257198	-1.858017
9	2.125111	-1.831963	-2.831084
9	4.118233	-1.293868	-2.187219
9	2.454862	0.023689	-1.755381
8	-1.046575	-3.025591	-0.172610
8	-0.399934	-1.079119	-1.930477
6	-0.794217	-3.371340	-1.541160
1	0.274918	-3.607968	-1.662726
1	-1.403912	-4.249411	-1.816278
6	-1.178631	-2.181790	-2.385501
1	-0.952135	-2.391670	-3.445596
1	-2.250439	-1.941020	-2.274875
6	-0.637257	-4.036353	0.761081
1	-1.211533	-4.958607	0.575171
1	0.441759	-4.226140	0.660054
1	-0.859764	-3.648861	1.761463
6	-0.563418	0.104446	-2.717280

1	-1.588149	0.493677	-2.625804
1	0.141868	0.845047	-2.330608
1	-0.315317	-0.120422	-3.767670
8	0.044671	0.956202	0.219651
6	1.078963	1.645048	0.252776
8	2.142186	1.305358	0.909939
6	1.140178	2.909371	-0.515051
6	-0.034748	3.415157	-1.101655
6	2.357533	3.598824	-0.657507
6	0.017407	4.606266	-1.825484
1	-0.979319	2.882503	-0.980703
6	2.401137	4.783519	-1.390701
1	3.260153	3.187885	-0.202877
6	1.231159	5.287959	-1.972834
1	-0.895869	5.003648	-2.274099
1	3.347262	5.316482	-1.510624
1	1.266906	6.219436	-2.543902
7	-1.073956	-1.134784	2.144453
7	-2.082483	-0.954066	2.787247
14	2.697026	0.988534	2.538912
7	-3.018922	-0.800159	3.425642
6	2.104952	-0.633012	3.230435
6	4.547009	1.034866	2.310408
6	1.987947	2.446455	3.484066
1	2.382101	-0.668909	4.298485
1	1.015271	-0.749557	3.146427
1	2.589744	-1.467924	2.708754
1	4.830820	0.235582	1.607638
1	4.887997	2.004461	1.914123
1	5.063145	0.850740	3.266953
1	2.302604	3.405183	3.041661
1	0.885553	2.409888	3.477340
1	2.317016	2.428764	4.536228

Structure S11. int3

E(B3LYP)sol = -6122.39328728 E(B3LYP)gas = -6122.39328728

6	0.686471	6.302697	0.136802
6	0.434338	5.156544	0.857970
6	-0.893916	4.640726	1.013946
6	-1.946407	5.379530	0.389169
6	-1.679278	6.532075	-0.328046
6	-0.363056	7.032947	-0.480233
1	1.719775	6.638380	0.031466
1	1.257289	4.602019	1.307633
1	-2.974076	5.017378	0.446957
1	-2.505628	7.070001	-0.802080
6	-1.089584	3.453797	1.742630

1	-0.202729	2.920732	2.089910	8	4.360049	1.861076	1.257698
6	-2.415601	2.802440	1.983275	8	3.120697	1.182718	-0.802361
1	-3.241528	3.525541	2.044427	6	3.546318	3.713304	-0.476648
1	-2.403537	2.235090	2.927175	9	3.626399	4.709335	0.409269
6	-0.143304	8.251074	-1.255989	9	4.709432	3.612769	-1.118487
1	-1.051490	8.694167	-1.682609	9	2.586918	3.987222	-1.352320
6	1.028813	8.870855	-1.495527	8	2.359068	-3.952537	-3.222997
1	1.980280	8.497855	-1.106896	16	1.883908	-3.883599	-1.835844
1	1.068350	9.782869	-2.096001	8	1.625074	-2.452471	-1.381228
6	-2.777708	1.806267	0.884510	8	0.811368	-4.781310	-1.409318
6	-4.073150	1.007911	1.196286	6	3.376276	-4.396266	-0.796132
9	-1.771364	0.898946	0.723535	9	4.515821	-4.034940	-1.387585
9	-2.963409	2.434336	-0.303108	9	3.370037	-5.715807	-0.652784
9	-3.812160	0.181698	2.235092	9	3.329801	-3.833996	0.418099
9	-5.036396	1.868795	1.584686	8	2.723667	-0.509310	-3.157105
6	-4.632605	0.184882	-0.018645	8	4.246608	-1.277886	-1.070543
6	-5.494515	-1.035288	0.426740	6	4.000270	-1.110323	-3.411401
9	-3.618903	-0.280133	-0.768591	1	3.871620	-2.199283	-3.514632
9	-5.382639	1.012431	-0.761735	1	4.423620	-0.693962	-4.342049
53	-6.525244	-1.959446	-1.285672	6	4.895496	-0.786940	-2.240584
9	-6.393769	-0.633534	1.328949	1	5.869346	-1.290630	-2.370937
9	-4.700091	-1.957846	0.988674	1	5.050213	0.301352	-2.140483
26	2.115284	-0.552712	-1.086379	6	1.734386	-0.811520	-4.152115
8	1.880999	2.265427	1.075744	1	2.058530	-0.406022	-5.124517
16	3.180497	2.108260	0.418310	1	1.586666	-1.899760	-4.217013

1	0.806485	-0.324859	-3.831468
6	5.042090	-1.173739	0.113632
1	5.240232	-0.119438	0.357239
1	4.470515	-1.632887	0.924934
1	5.982180	-1.731498	-0.029865
8	2.067609	-0.846679	0.919601
6	1.754715	-1.686212	1.782428
8	0.893390	-2.628413	1.581310
6	2.420894	-1.650123	3.105854
6	3.271377	-0.574242	3.420549
6	2.205398	-2.678144	4.040779
6	3.897695	-0.534084	4.666041
1	3.430252	0.226081	2.697331
6	2.840814	-2.633015	5.280795
1	1.550419	-3.510135	3.778236
6	3.685485	-1.560517	5.593949
1	4.552892	0.304651	4.911990
1	2.679923	-3.434384	6.005705
1	4.180514	-1.525472	6.567983
7	0.469282	0.344369	-1.391099
7	0.139139	1.506777	-1.443860
14	-0.807022	-2.943037	1.297268
7	-0.200374	2.596899	-1.512773
6	-1.369753	-2.381265	-0.379633
6	-0.884919	-4.793698	1.512524
6	-1.620762	-1.971999	2.677143
1	-2.464412	-2.497571	-0.423391
1	-1.134294	-1.323777	-0.561244
1	-0.908689	-2.994792	-1.163203
1	-0.255060	-5.269348	0.744844
1	-0.541449	-5.106027	2.511565
1	-1.919113	-5.150783	1.375936
1	-1.230182	-2.264498	3.664608
1	-1.447328	-0.894894	2.530293
1	-2.710587	-2.127798	2.667472

Structure S12. **^{7,5}MECP**

E(B3LYP)sol = -6127.14360046

6	0.602632	6.422682	0.144579
6	0.356641	5.205118	0.742116
6	-0.976336	4.709130	0.928576
6	-2.037707	5.539061	0.449522
6	-1.776922	6.765638	-0.137416
6	-0.456928	7.251807	-0.308677
1	1.639131	6.744807	0.021493
1	1.185190	4.587542	1.085466
1	-3.072588	5.202353	0.535869
1	-2.614089	7.379605	-0.484241

6	-1.163382	3.470067	1.570961	16	3.164569	2.141849	0.346013
1	-0.272041	2.892984	1.822264	8	4.344230	1.930942	1.194145
6	-2.483856	2.813965	1.823524	8	3.132934	1.188199	-0.857100
1	-3.317267	3.528159	1.872212	6	3.500666	3.736437	-0.577090
1	-2.465681	2.263675	2.778578	9	3.569778	4.745033	0.293866
6	-0.244518	8.557017	-0.930054	9	4.660313	3.642961	-1.225005
1	-1.161779	9.073577	-1.238384	9	2.530196	3.978582	-1.449466
6	0.928554	9.179450	-1.159182	8	2.429013	-4.024617	-3.132564
1	1.891439	8.740268	-0.885048	16	1.959584	-3.915847	-1.746213
1	0.956613	10.163936	-1.633240	8	1.684962	-2.471874	-1.340745
6	-2.840292	1.791347	0.747044	8	0.900263	-4.810651	-1.282941
6	-4.118351	0.980841	1.099849	6	3.462856	-4.375009	-0.697867
9	-1.821897	0.894172	0.593420	9	4.594650	-4.008547	-1.300669
9	-3.045159	2.386910	-0.453485	9	3.479629	-5.690233	-0.522506
9	-3.827998	0.198788	2.165873	9	3.408665	-3.783476	0.502359
9	-5.093160	1.837613	1.468754	8	2.772638	-0.571611	-3.150861
6	-4.683950	0.095182	-0.065829	8	4.283089	-1.260699	-1.033331
6	-5.528995	-1.108597	0.455220	6	4.056278	-1.170272	-3.378584
9	-3.676534	-0.400617	-0.805080	1	3.937160	-2.262859	-3.448304
9	-5.450827	0.877315	-0.839806	1	4.481226	-0.779815	-4.319589
53	-6.598282	-2.117171	-1.184893	6	4.939321	-0.801781	-2.212588
9	-6.409394	-0.671039	1.359105	1	5.918609	-1.300928	-2.318092
9	-4.716624	-2.001532	1.039322	1	5.083629	0.290232	-2.145119
26	2.140813	-0.558007	-1.087460	6	1.793490	-0.911398	-4.144457
8	1.856720	2.282084	0.989506	1	2.128089	-0.541943	-5.127290

1	1.646702	-2.001160	-4.170599
1	0.862238	-0.413681	-3.852659
6	5.068116	-1.110860	0.153380
1	5.252253	-0.047744	0.365766
1	4.497212	-1.552407	0.974431
1	6.016049	-1.660697	0.035033
8	2.061812	-0.814705	0.909491
6	1.789629	-1.657668	1.785940
8	0.929287	-2.605574	1.621405
6	2.505467	-1.611438	3.081438
6	3.329707	-0.509448	3.374940
6	2.366596	-2.658899	4.009664
6	4.008635	-0.462866	4.592167
1	3.428896	0.304281	2.656547
6	3.056607	-2.608430	5.220108
1	1.729727	-3.509201	3.762668
6	3.876075	-1.510212	5.511611
1	4.642444	0.396608	4.821544
1	2.958201	-3.425074	5.938925
1	4.413630	-1.470702	6.462546
7	0.501539	0.314063	-1.440950
7	0.154029	1.458883	-1.625764
14	-0.773057	-2.915557	1.314964
7	-0.202816	2.525497	-1.830414
6	-1.314310	-2.399738	-0.383577
6	-0.868993	-4.758403	1.582979
6	-1.594759	-1.896957	2.653426
1	-2.409591	-2.510375	-0.428717
1	-1.073725	-1.348930	-0.594517
1	-0.854636	-3.039607	-1.146528
1	-0.230518	-5.262237	0.840907
1	-0.546231	-5.043909	2.596777
1	-1.904004	-5.110362	1.438879
1	-1.216792	-2.160304	3.653862
1	-1.415950	-0.825633	2.473529
1	-2.684785	-2.049427	2.635428

Structure S13. **P**

E(B3LYP)sol = -1800.87612248 E(B3LYP)gas = -1799.10551758

6	-5.792091	-1.267751	0.868655
6	-4.593953	-0.578307	1.025854
6	-4.201845	0.409839	0.107307
6	-5.045301	0.693416	-0.971550
6	-6.247293	0.000039	-1.127456
6	-6.648799	-0.994748	-0.217519
1	-6.068164	-2.024559	1.605672
1	-3.951833	-0.808101	1.881949

1	-4.761919	1.469665	-1.684178
1	-6.894227	0.237925	-1.976529
6	-2.858955	1.099773	0.285421
1	-2.693428	1.271287	1.363094
6	-1.727067	0.181774	-0.227701
1	-1.756166	0.130810	-1.324244
1	-1.879819	-0.833694	0.164719
6	-7.928234	-1.693289	-0.431178
1	-8.486483	-1.361389	-1.314569
6	-8.462807	-2.665935	0.322179
1	-7.972112	-3.055701	1.218478
1	-9.425808	-3.111388	0.061195
6	-0.343228	0.623684	0.213678
6	0.751963	-0.406027	-0.187836
9	-0.312485	0.759849	1.566670
9	-0.009946	1.826025	-0.323377
9	0.547472	-1.525086	0.540978
9	0.590731	-0.712662	-1.492251
6	2.220349	0.093899	0.010801
6	3.266389	-1.062228	-0.035340
9	2.327193	0.705989	1.201853
9	2.488455	0.970846	-0.969449
53	5.324510	-0.268067	-0.052765
9	3.066368	-1.796067	-1.134603
9	3.116734	-1.840595	1.037289
7	-1.838301	4.299250	0.498924
7	-2.307653	3.343663	0.101284
7	-2.850411	2.384684	-0.436628

Structure S14. **TS2**

E(B3LYP)sol = -3183.73585909 E(B3LYP)gas = -3180.98365996

6	2.250876	5.632161	0.407124
6	1.808086	4.438733	0.958797
6	1.605713	3.291460	0.160397
6	1.850036	3.401038	-1.222641
6	2.291570	4.598012	-1.773124
6	2.505167	5.742841	-0.977022
1	2.402624	6.493326	1.060614
1	1.613486	4.380749	2.033118
1	1.691161	2.542938	-1.877850
1	2.478014	4.655744	-2.848848
6	1.126699	2.048193	0.788703
1	1.221361	2.071105	1.879296
6	1.565047	0.706734	0.226618
1	1.396027	0.629691	-0.854505
1	0.999620	-0.104916	0.704337
6	2.973928	6.981412	-1.614058

1	3.119269	6.912101	-2.698388
6	3.234486	8.155467	-1.016786
1	3.116785	8.309366	0.059382
1	3.580238	9.014099	-1.597285
6	3.042053	0.433729	0.499871
6	3.439197	-1.013992	0.088506
9	3.304457	0.579950	1.823413
9	3.840786	1.296367	-0.177520
9	2.814010	-1.866633	0.927734
9	2.986056	-1.239843	-1.163746
6	4.977858	-1.293857	0.099015
6	5.317890	-2.815378	0.053566
9	5.519061	-0.777878	1.214941
9	5.509328	-0.690916	-0.976614
53	7.482427	-3.134756	-0.233518
9	4.649794	-3.387733	-0.952657
9	4.948956	-3.388202	1.199618
6	-4.103450	0.089943	0.091349
9	-3.686180	0.112033	-1.187936
9	-3.347857	-0.767553	0.799503
6	-3.938770	1.495380	0.676226
9	-4.492281	2.440335	-0.065315
9	-4.331537	1.584824	1.935936
53	-1.244763	2.050578	0.633814
6	-5.582921	-0.423536	0.133836
6	-5.810757	-1.753215	-0.643657
53	-7.874579	-2.491235	-0.356758
9	-6.376379	0.522212	-0.402048
9	-5.912786	-0.601393	1.423982
9	-4.951135	-2.677176	-0.208386
9	-5.605216	-1.549291	-1.945093

Frequencies -- -94.0418

Red. masses -- 29.1981

Frc consts -- 0.1521

IR Inten -- 42.5544

Structure S15. P'

E(B3LYP)sol = -1934.42957549 E(B3LYP)gas = -1932.83797974

6	-4.133666	2.597773	1.017974
6	-3.634576	1.319829	1.249908
6	-3.161015	0.522096	0.194182
6	-3.217228	1.043696	-1.107791
6	-3.718358	2.320538	-1.339666
6	-4.186380	3.130439	-0.284920
1	-4.486600	3.189260	1.865041
1	-3.604334	0.931239	2.271508
1	-2.877301	0.441270	-1.953215

1	-3.751555	2.705730	-2.362443
6	-2.612039	-0.838162	0.484232
1	-2.527444	-0.995070	1.564996
6	-1.291540	-1.206884	-0.190725
1	-1.337149	-1.090604	-1.280818
1	-1.040883	-2.255712	0.019328
6	-4.703401	4.475158	-0.587857
1	-4.687135	4.741679	-1.651225
6	-5.177633	5.380994	0.280933
1	-5.227493	5.196378	1.357658
1	-5.536656	6.353553	-0.064196
6	-0.132008	-0.362093	0.328588
6	1.235426	-0.896320	-0.189503
9	-0.103822	-0.392684	1.686300
9	-0.246844	0.933945	-0.052834
9	1.456837	-2.095146	0.390957
9	1.142630	-1.080782	-1.524272
6	2.448189	0.053526	0.080118
6	3.825594	-0.655648	-0.100736
9	2.380696	0.519736	1.338149
9	2.363814	1.078562	-0.782807
53	5.483241	0.798042	-0.006164
9	3.850835	-1.277624	-1.283576
9	3.992253	-1.558132	0.866534
53	-4.119076	-2.414613	-0.079140

Structure S16. octa-1,7-diene

E(B3LYP)sol = -313.381642219 E(B3LYP)gas = -313.029913534

6	-0.667017	-0.345934	0.143405
1	-0.836640	-0.388393	1.234311
1	-0.614639	-1.397334	-0.195000
6	-1.866856	0.344739	-0.524646
1	-1.681925	0.390013	-1.615041
1	-1.934326	1.390617	-0.177208
6	-3.168677	-0.363054	-0.273977
1	-3.221080	-1.400070	-0.633690
6	-4.227740	0.155502	0.354094
1	-4.219735	1.183309	0.733753
1	-5.143140	-0.422423	0.510469
6	0.666923	0.346215	-0.143529
1	0.614590	1.397613	0.194898
1	0.836493	0.388676	-1.234444
6	1.866740	-0.344479	0.524472
1	1.934071	-1.390446	0.177257
1	1.681953	-0.389521	1.614902
6	3.168614	0.363105	0.273550
1	3.220786	1.400518	0.632160

6	4.228003	-0.156091	-0.353433
1	5.143439	0.421726	-0.509995
1	4.220215	-1.184304	-0.731994

Structure S17. **TS1"**

E(B3LYP)sol = -353.234366225 E(B3LYP)gas = -352.835315731

6	1.354058	0.247460	-0.160427
1	1.410198	1.070433	0.574594
1	1.255138	0.732455	-1.149268
6	2.664165	-0.555377	-0.116142
1	2.593291	-1.381410	-0.849564
1	2.776549	-1.028778	0.875019
6	3.876330	0.277011	-0.426419
1	3.884027	0.751619	-1.417510
6	4.904798	0.491817	0.398889
1	4.938441	0.043406	1.398084
1	5.752896	1.118991	0.109395
6	0.112414	-0.603405	0.113660
1	0.210877	-1.088348	1.102457
1	0.056224	-1.426463	-0.621276
6	-1.198183	0.199300	0.071102
1	-1.309962	0.674421	-0.919743
1	-1.120343	1.029734	0.801523
6	-2.412790	-0.623767	0.381613
1	-2.418274	-1.128597	1.356654
6	-3.514089	-0.715983	-0.411456
1	-4.317442	-1.416330	-0.171907
1	-3.491393	-0.335677	-1.437025
6	-4.955898	1.073684	0.124685
1	-5.151201	0.855390	1.176519
1	-4.294272	1.914600	-0.093491
1	-5.759581	0.870112	-0.587484

Frequencies -- -389.5851

Red. masses -- 10.6222

Frc consts -- 0.9499

IR Inten -- 0.7675

Structure S18. **int1"**

E(B3LYP)sol = -353.280079319 E(B3LYP)gas = -352.887509549

6	1.322518	-0.082610	0.313818
1	1.312032	-1.144771	0.009620
1	1.300798	-0.085586	1.419470
6	2.631622	0.563615	-0.167233
1	2.627530	1.628591	0.134679

1	2.667217	0.553846	-1.270774
6	3.857980	-0.102194	0.390507
1	3.941922	-0.098782	1.486205
6	4.814525	-0.698210	-0.327024
1	4.770938	-0.730591	-1.421400
1	5.677981	-1.172942	0.147866
6	0.069932	0.617037	-0.216284
1	0.093260	0.622650	-1.321681
1	0.080822	1.678572	0.090501
6	-1.238488	-0.028603	0.253889
1	-1.266907	-0.052957	1.361790
1	-1.228173	-1.102534	-0.043363
6	-2.472499	0.635161	-0.262608
1	-2.413278	1.152906	-1.228033
6	-3.823951	0.322996	0.296204
1	-4.525493	1.144226	0.066026
1	-3.764097	0.261787	1.399461
6	-4.420987	-0.999682	-0.234118
1	-4.533614	-0.971303	-1.330128
1	-3.771066	-1.855154	0.011953
1	-5.413781	-1.193029	0.204907

Structure S19. **TS3**

E(B3LYP)sol = -1562.68834528 E(B3LYP)gas = -1561.17915042

6	6.510653	-0.577759	0.154268
1	6.344013	-1.180874	-0.756167
1	6.143748	-1.193746	0.995912
6	8.017848	-0.328639	0.323867
1	8.171472	0.283701	1.233075
1	8.392706	0.272621	-0.522928
6	8.814159	-1.597708	0.442975
1	8.551164	-2.244323	1.291586
6	9.776048	-1.993389	-0.395482
1	10.068818	-1.383692	-1.257524
1	10.310239	-2.937118	-0.252870
6	5.690208	0.711039	0.073822
1	6.055738	1.327427	-0.768065
1	5.855643	1.314198	0.984508
6	4.183891	0.458728	-0.097632
1	3.804266	-0.146784	0.743406
1	4.029194	-0.153093	-1.007859
6	3.379100	1.715719	-0.225547
1	3.663513	2.393134	-1.041344
6	2.305011	2.026846	0.535537
1	1.775217	2.975107	0.417291
1	2.038667	1.420662	1.406655

6	0.545227	0.834208	-0.652696
6	-0.628458	0.804452	0.307053
9	1.085689	-0.351973	-0.894617
9	0.316782	1.500320	-1.774671
9	-0.246816	0.124566	1.410962
9	-0.925545	2.076642	0.648848
6	-1.921569	0.141428	-0.270401
6	-3.067628	-0.043618	0.764168
9	-1.584390	-1.068783	-0.755178
9	-2.355711	0.918668	-1.277877
53	-4.889884	-0.841142	-0.204149
9	-3.352425	1.132454	1.328397
9	-2.678416	-0.895731	1.713538

Frequencies -- -164.5514

Red. masses -- 7.0940

Frc consts -- 0.1132

IR Inten -- 21.4162

Structure S20. int4

E(B3LYP)sol = -1562.73243844 E(B3LYP)gas = -1561.22853677

6	6.466003	-0.336229	0.337542
1	6.105857	-1.372550	0.208279
1	6.430704	-0.138050	1.424852
6	7.920834	-0.245065	-0.149671
1	8.267510	0.798690	-0.024152
1	7.964091	-0.458849	-1.232025
6	8.848980	-1.165829	0.591613
1	8.917011	-0.998276	1.675485
6	9.560247	-2.156651	0.046473
1	9.520404	-2.363855	-1.028711
1	10.211043	-2.796179	0.649636
6	5.523983	0.628260	-0.384868
1	5.560374	0.431473	-1.472069
1	5.882020	1.665204	-0.253103
6	4.071075	0.529118	0.093734
1	4.016677	0.718183	1.183528
1	3.724538	-0.521312	-0.020197
6	3.131221	1.439707	-0.620761
1	3.324286	1.675251	-1.672422
6	1.785775	1.778298	-0.068047
1	1.392692	2.709637	-0.502106
1	1.817956	1.899150	1.027663
6	0.747993	0.688163	-0.350510
6	-0.648444	1.026176	0.244027
9	1.151294	-0.491699	0.189175
9	0.603760	0.502928	-1.687502
9	-0.538568	0.999546	1.590589

9	-0.982344	2.280797	-0.129674
6	-1.803332	0.073332	-0.208167
6	-3.083785	0.210092	0.671773
9	-1.387445	-1.202252	-0.140600
9	-2.109383	0.377162	-1.479966
53	-4.764611	-0.932950	-0.191805
9	-3.427547	1.498535	0.759774
9	-2.835777	-0.255947	1.896226

Structure S21. **TS4**

E(B3LYP)sol = -3109.90018507 E(B3LYP)gas = -3107.22935428

6	1.674736	2.808919	-0.193794
1	1.379101	3.533220	-0.973832
1	1.888784	1.863174	-0.718450
6	2.957112	3.298449	0.496716
1	3.247082	2.548326	1.255167
1	2.757927	4.239131	1.039684
6	4.102468	3.486688	-0.458310
1	4.403153	2.593235	-1.017731
6	4.753059	4.633385	-0.674272
1	4.487660	5.552658	-0.140274
1	5.579953	4.696316	-1.387588
6	0.507674	2.600648	0.777689
1	0.248177	3.568187	1.238945
1	0.841782	1.954593	1.607575
6	-0.746129	1.986571	0.111942
1	-0.624322	1.940266	-0.984404
1	-1.618542	2.648793	0.272058
6	-1.166377	0.633805	0.618542
1	-1.203762	0.548223	1.711952
6	-2.303926	-0.079764	-0.075528
1	-2.340203	-1.137579	0.219025
1	-2.199089	-0.036037	-1.169794
6	-3.668486	0.513254	0.278701
6	-4.835831	-0.295882	-0.359610
9	-3.767474	1.793968	-0.161832
9	-3.844423	0.525852	1.624680
9	-4.756341	-0.135420	-1.697734
9	-4.658452	-1.603466	-0.075191
6	-6.261643	0.110163	0.140426
6	-7.403386	-0.451594	-0.761936
9	-6.367072	1.449096	0.160832
9	-6.406420	-0.368711	1.386386
53	-9.380345	-0.097388	0.151084
9	-7.225801	-1.764701	-0.935423
9	-7.365953	0.150967	-1.951055
6	4.016279	-0.600807	0.029909

9	3.730367	0.167085	-1.041705
9	3.808649	0.107739	1.155550
6	3.059593	-1.812462	0.018973
9	3.118602	-2.463856	-1.138326
9	3.323558	-2.644680	1.023037
53	0.788524	-0.934766	0.299986
6	5.531971	-0.985772	-0.018874
6	6.479796	0.242027	-0.189876
53	8.595320	-0.374649	-0.068013
9	5.729866	-1.822369	-1.052054
9	5.830721	-1.613849	1.129847
9	6.227585	1.139274	0.765142
9	6.265412	0.807771	-1.380882

Frequencies -- -150.6131

Red. masses -- 21.7262

Frc consts -- 0.2904

IR Inten -- 1.3803

Structure S22. P"

E(B3LYP)sol = -1860.59772634 E(B3LYP)gas = -1859.08278956

6	-5.461531	1.512684	0.247725
1	-5.286342	2.203618	1.091784
1	-5.604275	0.513521	0.693489
6	-6.742911	1.930214	-0.489206
1	-6.904273	1.228384	-1.329856
1	-6.608533	2.930034	-0.938559
6	-7.956603	1.924711	0.396901
1	-8.205356	0.956077	0.851978
6	-8.719176	2.985074	0.677884
1	-8.506262	3.971249	0.250396
1	-9.585910	2.910066	1.340839
6	-4.227558	1.495290	-0.659703
1	-4.072268	2.510001	-1.063515
1	-4.430980	0.855498	-1.536493
6	-2.936074	1.022201	0.042660
1	-3.073200	0.995449	1.137160
1	-2.133645	1.755733	-0.136024
6	-2.378823	-0.317525	-0.423515
1	-2.248573	-0.323152	-1.513805
6	-1.080282	-0.765723	0.252193
1	-0.823565	-1.781541	-0.074090
1	-1.183871	-0.783927	1.346863
6	0.114285	0.123982	-0.078455
6	1.459691	-0.523882	0.366208
9	0.018096	1.326580	0.547485
9	0.182983	0.361379	-1.415190
9	1.447651	-0.598243	1.714238

9	1.521598	-1.777615	-0.130322
6	2.742108	0.234932	-0.111870
6	4.033106	-0.230259	0.630715
9	2.594756	1.553150	0.098567
9	2.882456	0.005824	-1.427579
53	5.833899	0.658418	-0.284379
9	4.122697	-1.562260	0.576353
9	3.970645	0.147408	1.908164
53	-3.854244	-1.967800	-0.132128

Supplemental References

Becke, A. D. 1993. Density ‐ functional thermochemistry. III. The role of exact exchange. *The Journal of Chemical Physics,* 98**,** 5648-5652.

Besalú, E. & Bofill, J. M. 1998. On the automatic restricted-step rational-function-optimization method. *Theoretical Chemistry Accounts,* 100**,** 265-274.

Frisch, M. J., Trucks, G. W., Schlegel, H. B., Scuseria, G. E., Robb, M. A., Cheeseman, J. R., Scalmani, G., Barone, V., Mennucci, B., Petersson, G. A., Nakatsuji, H., Caricato, M., Li, X., Hratchian, H. P., Izmaylov, A. F., Bloino, J., Zheng, G., Sonnenberg, J. L., Hada, M., Ehara, M., Toyota, K., Fukuda, R., Hasegawa, J., Ishida, M., Nakajima, T., Honda, Y., Kitao, O., Nakai, H., Vreven, T., Montgomery Jr., J. A., Peralta, J. E., Ogliaro, F., Bearpark, M. J., Heyd, J., Brothers, E. N., Kudin, K. N., Staroverov, V. N., Kobayashi, R., Normand, J., Raghavachari, K., Rendell, A. P., Burant, J. C., Iyengar, S. S., Tomasi, J., Cossi, M., Rega, N., Millam, N. J., Klene, M., Knox, J. E., Cross, J. B., Bakken, V., Adamo, C., Jaramillo, J., Gomperts, R., Stratmann, R. E., Yazyev, O., Austin, A. J., Cammi, R., Pomelli, C., Ochterski, J. W., Martin, R. L., Morokuma, K., Zakrzewski, V. G., Voth, G. A., Salvador, P., Dannenberg, J. J., Dapprich, S., Daniels, A. D., Farkas, , Foresman, J. B., Ortiz, J. V., Cioslowski, J. & Fox, D. J. 2013. Gaussian 09. Gaussian 09, Revision D.01 ed. Wallingford, CT, USA: Gaussian, Inc.

Fukui, K. 1981. The path of chemical reactions - the IRC approach. *Accounts of Chemical Research,* 14**,** 363-368.

Gauler, R. & Risch, N. 1998. New Heck-type coupling reactions of natural tetrapyrroles - Synthesis of porphyrinoligomers bridged by divinyl- and trivinylbenzene. *European Journal of Organic Chemistry***,** 1193-1200.

Grimme, S., Antony, J., Ehrlich, S. & Krieg, H. 2010. A consistent and accurate ab initio parametrization of density functional dispersion correction (DFT-D) for the 94 elements H-Pu. *The Journal of Chemical Physics,* 132**,** 154104.

Grimme, S., Ehrlich, S. & Goerigk, L. 2011. Effect of the damping function in dispersion corrected density functional theory. *Journal of Computational Chemistry,* 32**,** 1456-1465.

Harvey, J. N., Aschi, M., Schwarz, H. & Koch, W. 1998. The singlet and triplet states of phenyl cation. A hybrid approach for locating minimum energy crossing points between non-interacting potential energy surfaces. *Theoretical Chemistry Accounts,* 99**,** 95-99.

Lee, C., Yang, W. & Parr, R. G. 1988. Development of the Colle-Salvetti correlation-energy formula into a functional of the electron density. *Physical Review B,* 37**,** 785-789.

Marenich, A. V., Cramer, C. J. & Truhlar, D. G. 2009. Universal Solvation Model Based on Solute Electron Density and on a Continuum Model of the Solvent Defined by the Bulk Dielectric Constant and Atomic Surface Tensions. *The Journal of Physical Chemistry B,* 113**,** 6378-6396.

Tello-Aburto, R., Lucero, A. N. & Rogelj, S. 2014. A catalytic approach to the MH-031 lactone: application to the synthesis of geralcin analogs. *Tetrahedron Letters,* 55**,** 6266-6268.

Weigend, F. 2006. Accurate Coulomb-fitting basis sets for H to Rn. *Physical Chemistry Chemical Physics,* 8**,** 1057-1065.

Weigend, F. & Ahlrichs, R. 2005. Balanced basis sets of split valence, triple zeta valence and quadruple zeta valence quality for H to Rn: Design and assessment of accuracy. *Physical Chemistry Chemical Physics*, 7**,** 3297-3305.